Role of C.T Angiography In Diagnosis of Extracranial Carotid Artery Diseases

Theses

Submitted for the partial fulfillment of the master degree in Radio-Diagnosis

تمت مناقشة الرسالة
يوم ٢٤/١١/٢٠٠٥
أمام لجنة الحكم
مكونة من
NP معوض
NP [illegible]
P/ مصطفى فاضل

By

Mahmoud Ebrahim El-Shamy

(M.B.B.Ch)

Under Supervision of

Prof.Dr.Mostafa Fadel Sonbol

Professor of Radio-Diagnosis
Faculty of Medicine
Al-Azhar University

Prof.Dr.Amr Mahmoud Zayed

Professor of radio-diagnosis
Faculty of medicine
Al-Azhar University

Prof. Dr.Hany Hafez Sherif

Assistant Professor of Radio-Diagnosis
Faculty of Medicine
Al-Azhar University

Faculty of Medicine
Al-Azhar University
2005

المنارة للاستشارات

www.manaraa.com

بسم الله الرحمن الرحيم

(قالوا سبحانك لا علم لنا الا ما علمتنا
انك أنت العليم الحكيم)

صدق الله العظيم
(أيه ٣٢ البقرة)

رات
:om

Acknowledgement

-ALL THANKS TO ALLAH-

Words fail to express my deepest gratitude and thanks to **Prof. Dr. Mostafa Fadel Sonbol** Professor of Radio-Diagnosis, Faculty of Medicine, Al-Azhar University, for his help and guidance throughout this work.

A special note of gratitude sent to **Prof. Dr. Amr Mahmoud Zayed** Professor of Radio-Diagnosis, Faculty of Medicine, Al-Azhar University, for his consult guidance. He has been very kind, generous with scientific advice.

My much appreciation and gratitude is forwarded to **Prof. Dr. Hany Hafez Sherif,** Assistant professor of Radio-Diagnosis, Faculty of Medicine Al-Azhar University, for his valuable time, consult guidance and valuable directions.

Last, but not least, I must express my sincere gratitude and deep appreciation to every one who helped me in this work, specially Dr. Maged Ali , Assistant Lecture of Radio- Diagnosis, for his great help.

رات
:om

TO MY PARENT

رات
:com

Contents

رات
:om

List of abbreviations

3D	Three-dimensional
AVM	Arteriovenous malformation
CCA	Common carotid artery
CT	Computed tomography
CTA	Computed tomography angiography
DSA	Digital subtraction angiography
ECA	External carotid artery
E.D.V	End diastolic velocity
ICA	Internal carotid artery
IJV	Internal jugular vein
IMT	Intima media thickness
IV	Intravenous
Lt	Left
MIP	Maximum intensity projection
MPR	Multiplanar reconstruction
NASCET	North American Symptomatic Carotid Endarterectomy
P.S.V	Peak systolic velocity
ROI	Region of interest
RT	Right
SSD	Shaded surface display
TIAs	Transient ischemic attacks
US	Ultrasonography

رات
:om

INTRODUCTION

رات

:om

Introduction

Stroke remains the third leading cause of death all over the world and survivors have significant residual morbidity rates. More than 500,000 new strokes are caused by extra-cranial carotid artery disease and therefore potentially preventable **(Marek et al., 1996).**

Prevention of stroke is aided by determination of the degree of carotid artery stenosis and progression of arterial sclerosis **(Sameshima et al., 1999)**.

The degree of stenosis of the internal carotid is associated with the risk of stoke. Finding in studies from the North American Symptomatic Carotid Endarterectomy Trial (NASCET) and the European Carotid Surgery Trial have proved that symptomatic patients with severe stenosis (70-99%) can benefit from carotid endarterectomy. Carotid endarterectomy may also useful for treating asymptomatic patients with carotid artery stenosis greater than 60%. In addition, the finding in NASCET studies indicate that some patients with stenosis as low as 50% can benefit from carotid endarterectomy **(Tshinorietal., 2001).**

رات

:om

Hence, accurate examination of the carotid artery is necessary to facilitate appropriate treatment and to prevent unnecessary intervention **(Scott et al., 1998)**.

Carotid digital subtraction is widely accepted as the gold standard for the assessment of carotid artery disease. This examination, however, is invasive and has its own risk (1.8% systemic complications and 0.3% risk of permanent neurological sequelae). Accurate non-invasive studies have been developed with comparable results to angiography e.g. Carotid duplex sonography, magnetic resonance (MR) angiography and computed tomography (CT) angiography **(Scott et al., 1998)**.

CT angiography is new non-invasive vascular imaging technique in which angiographic images are produced by performing three-dimensional (3D) display or reconstruction of vessel anatomy as described on the overlapping images obtained with helical CT **(Evan et al., 1993)**.

Helical CT with 3D reconstruction produces angiographic images and is accurate in evaluating the degree of ICA stenosis despite the radiation dose and need for iodinated contrast material administration. This technique is based on a rapid acquisition of the entire volume owing to the continuous rotation of the gantry and simultaneous displacement of the

:om

examination table. Data acquisition by using narrow collimation can be reconstructed with overlapping section; this provides high spatial resolution **(Tshinorietal., 2001).**

CT angiography (CTA) can be performed as an outpatient procedure and the examination takes only few minutes, requires only intravenous (I.V) contrast injection and involves less radiation than angiography. The raw data can be edited retrospectively and any additional views can be reconstructed without additional contrast injections **(Link et al., 1997)**.

The high level of accuracy in assessment of vascular stenosis has been documented by CT angiographic studies. This high accuracy has shown CTA to be superior to duplex sonography, which is considered the primary screening examination for carotid artery disease **(Scott et al., 1998) .**

In particular, helical CT angiography provides more global view of the carotid circulation including the distal cervical segment which is not accurately evaluated when using Doppler sonography **(Michael et al., 1993)**.

CT angiography can grade all severe stenosis and occlusions and showed a good correlation with DSA **(Link et al., 1997).**

رات
:om

Aim of the work

Evaluation the role of helical CT angiography in diagnosis of extracranial carotid artery diseases.

رات
:om

Carotid vascular anatomy

The Common carotid artery is a large bilateral vessel supplying head and neck; it ascends to just above the level of thyroid cartilage's upper border, where it divides into an external carotid, supplying the exterior of the head ,face and most of the neck, and an internal carotid, supplying the cranial and orbital content **(William et al., 1995).**

The right and left carotid arteries differ in length and origin. The right carotid exclusively cervical, originates from the Brachiocephalic trunk behind the right sternoclavicular joint, the left carotid originates directly from aortic arch immediately posterolateral to the Brachiocephalic trunk and therefore has both thoracic and cervical parts.

The thoracic part of left common carotid artery

Ascends until the level of the left sternoclavicular joint where it enters the neck. It is 20-25mm long and it lies at first in front of the trachea then it inclines to the left

Relations:-

Anteriorly, are the sternohyoid and sternothyroid, the anterior parts of left pleura and lung, the left Brachiocephalic

رات
:om

vein and the thymic remnants, separating it from the manubrium; ***Posteriorly*** ,are the trachea, left subclavian artery, left borders of the oesophagus, left recurrent laryngeal nerve and the thoracic duct. ***To the right***, are (below) the Brach:ocephalic trunk and (above) the trachea, inferior thyroid veins and thymic remnants. ***To left***, are the left vagus and left phrenic nerves, left pleura and lung.

Cervical part of both common carotid arteries

Following a similar course, it ascends, diverging laterally from behind the sternoclavicular joint to the thyroid cartilage upper border, where it divides into external and internal carotid arteries (Fig. 1). At its division the vessels have dilatation, the carotid sinus, usually involving or restricted to the beginning of the internal carotid.

In the lower neck, the common carotids are separated by a narrow gap into which projects the trachea, above this the thyroid gland, larynx and pharynx project between them. Each is contained in a carotid sheath, which is continuous with deep cervical fascia and of loose texture, though, that actually around the artery is denser. This sheath encloses also the internal jugular vein and vagus nerve, the vein lies laterally to the artery, the nerve between them and posterior to both **(Williams et at., 1995).**

رات
:om

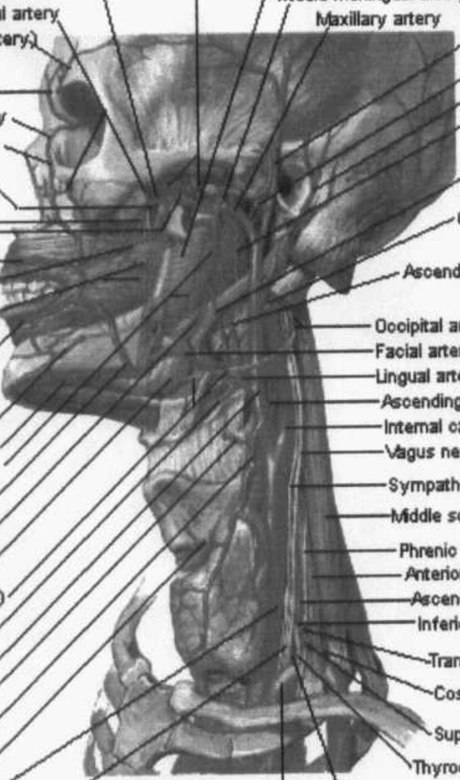

Figure (1) Extracranial cerebrovascular anatomy

Quoted from (William et al., 1995)

Relation:-

The artery is crossed ***anterolaterally***, at the level of cricoid cartilage, by intermediate tendon (sometimes the posterior belly of omohyoid). Below this muscle, it is sited deeply, covered by skin, superficial fascia, platysma, deep cervical fascia, the sternomastoid, sternohyoid and sternothyroid. Above the omohyoid, it is more superficial, covered merely by skin, superficial fascia, platysma, deep cervical fascia and the medial margin of sternomastoid and is crossed obliquely from its medial to lateral side by sternomastoid branch of superior

www.manaraa.com

thyroid artery. In front of, or embedded in the carotid sheath is the superior root of the ansa cervicalis, joined by its inferior root from the second and third cervical nerves and crossing the vessel obliquely. The superior thyroid vein usually crosses near the artery end, the middle thyroid vein a little below cricoid level; the anterior jugular vein crosses it above the clavicle, separated by sternohyoid and sternothyroid.

Posteriorly, are the fourth to sixth cervical transverse processes, and attached to them the longus colli longus capitis and tindinous slips of scalenus anterior; the sympathetic trunk and ascending cervical artery are between the common carotid artery and the muscle. Below the level of the sixth cervical vertebra, the artery is in an angle between the scalenus anterior and longus colli, anterior to the vertebral vessels, inferior thyroid and subclavian arteries, sympathetic trunk and, on left thoracic duct.

Medially, are the esophagus, trachea, inferior thyroid artery and recurrent laryngeal nerve and, at higher level, the larynx and pharynx; the thyroid gland overlaps it anteromedially. ***Laterally,*** is the internal jugular vein, which in the lower neck is also anterior to the artery; posterolateral in the angle between artery and vein is the vagus nerve.

رات
:om

On the right, low in the neck, the recurrent laryngeal crosses obliquely behind the artery, the right internal jugular vein diverges from it below but the left vein approaches and often overlaps its artery.

Variation: - In about 12%, the right common carotid artery arises above the level of the sternoclavicular joint or may be a separate branch from the aorta. The left common carotid artery varies in origin more than right; it may arise with the Brachiocephalic. Division of the common carotid may occur higher, near the level of the hyoid bone, more rarely at lower level alongside the larynx. Very rarely, it ascends without division, either the external or the internal carotid being absent. Rarely, also, it is replaced by separate external and internal carotid arteries arising directly from the aorta bilaterally.

The common carotid usually has no branches but the vertebral, superior thyroid or its laryngeal branch, ascending pharyngeal, inferior thyroid or occipital may be branches of it **(Williams et at., 1995).**

The external carotid artery (ECA)

Commences at the bifurcation of the common carotid, near the greater horn of the hyoid bone (fig. 2). At first, it slopes upward in front of internal carotid artery, passes deep to the posterior belly of the digastric and stylohyoid, above which it

ارات
:om

pierces the deep lamina of the parotid fascia and enters the gland. It divides within the gland behind the neck of mandible into maxillary and superficial temporal arteries.

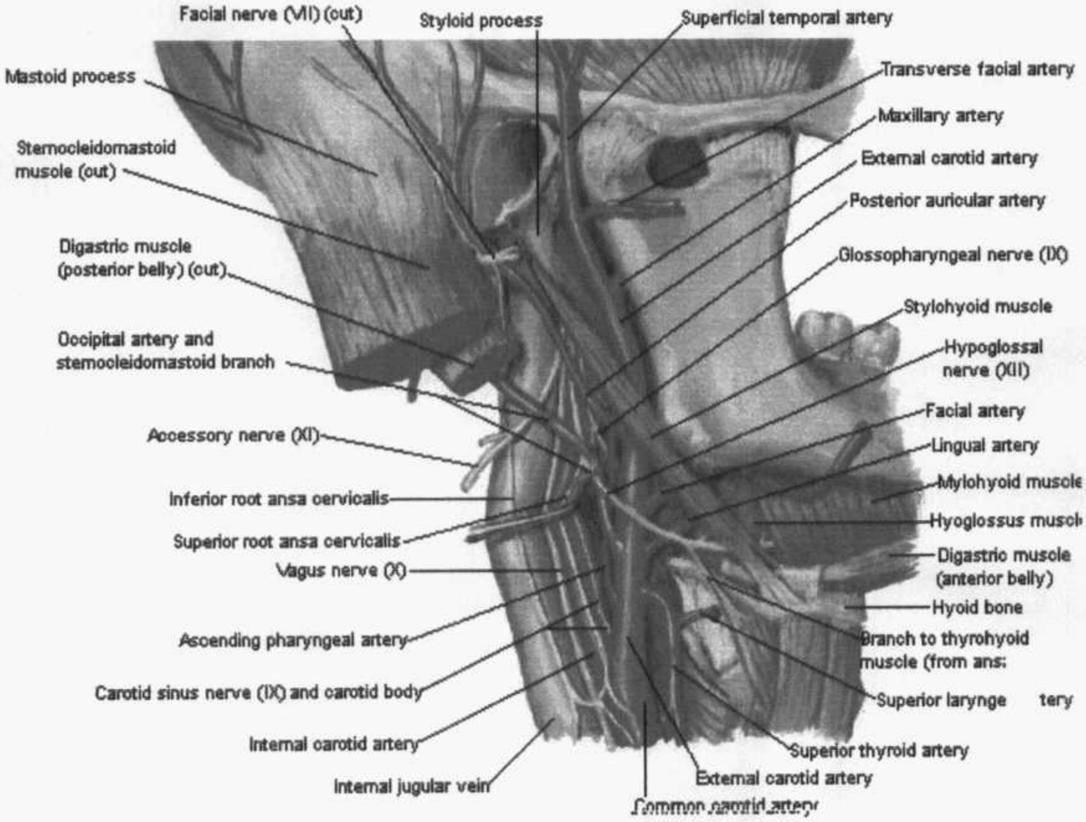

Figure (2) External carotid artery (Quoted from :William et al., 1995)

Branches of external carotid artery

1. From the anterior surface: superior thyroid, lingual and facial arteries (from below upwards).
2. From the posterior surface: occipital and posterior auricular arteries.

المنارة للاستشارات
www.manaraa.com

3. From the medial surface: ascending pharyngeal artery (Fig.3) **(Williams et al., 1995).**

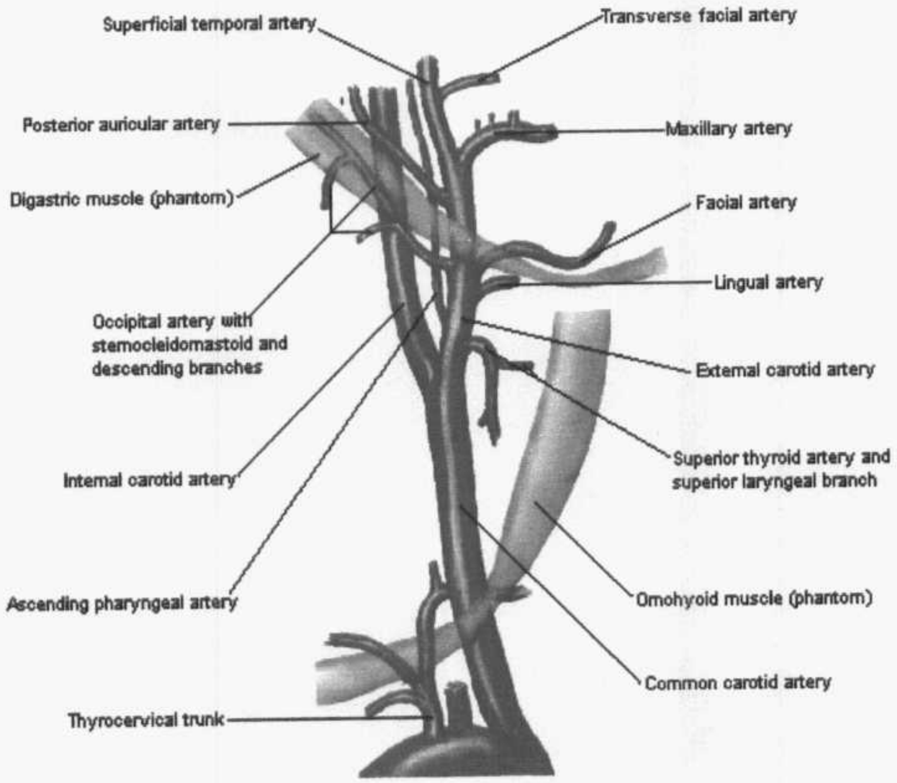

Figure (3) External carotid artery branches

Quoted from (William et al., 1995)

Internal carotid artery (ICA)

The internal carotid artery supplies most of the ipsilateral cerebral hemisphere, eye, accessory organs, forehead and the nose. From the carotid bifurcation, where it usually has carotid sinus. It ascends to the cranial base, enters the cranial cavity through the carotid canal and turns anteriorly through the cavernous sinus in the carotid groove on the side of the sphenoid

المنارة للاستشارات
www.manaraa.com

body, ending below the anterior perforating substance by division into the anterior and middle cerebral arteries (Fig.4).

Cervical part

This section begins at the carotid bifurcation and ascends in front of the upper three cervical transverse processes to the inferior aperture of the carotid canal in the petrous temporal bone. It is superficial at first in the carotid triangle, and then passes deeper, medial to posterior belly of digastric. Near the skull, the internal jugular vein and vagus nerve are lateral; the external carotid is first anteromedial but then curves backwards to become superficial. The artery has many other variations; **posteriorly**, it adjoins the longus capitis, with superior cervical sympathetic ganglion between them and the superior laryngeal nerve crossing obliquely behind it. **Medially,** the pharyngeal wall is separated by fat and pharyngeal veins from the ascending pharyngeal artery and superior laryngeal nerve. **Anterolaterally,** the artery is covered by the sternomastoid, below the digastric muscle, the hypoglossal nerve and superior root of the ansa cervicalis and the lingual and facial veins are superficial. At the level of the digasrtic it is crossed by the stylohyoid muscle and the occipital and posterior auricular arteries. Above the digastric it is separated from the external carotid by styloid process, styloglossus and stylopharyngeus, glossopharyngeal nerve, vagal pharyngeal branch and the deeper

المنارة للاستشارات
www.manaraa.com

part of the parotid gland. At the base of the skull the glossopharyngeal, vagus, accessory and hypoglossal nerves are between the internal carotid artery and the internal jugular vein, which here has become posterior.

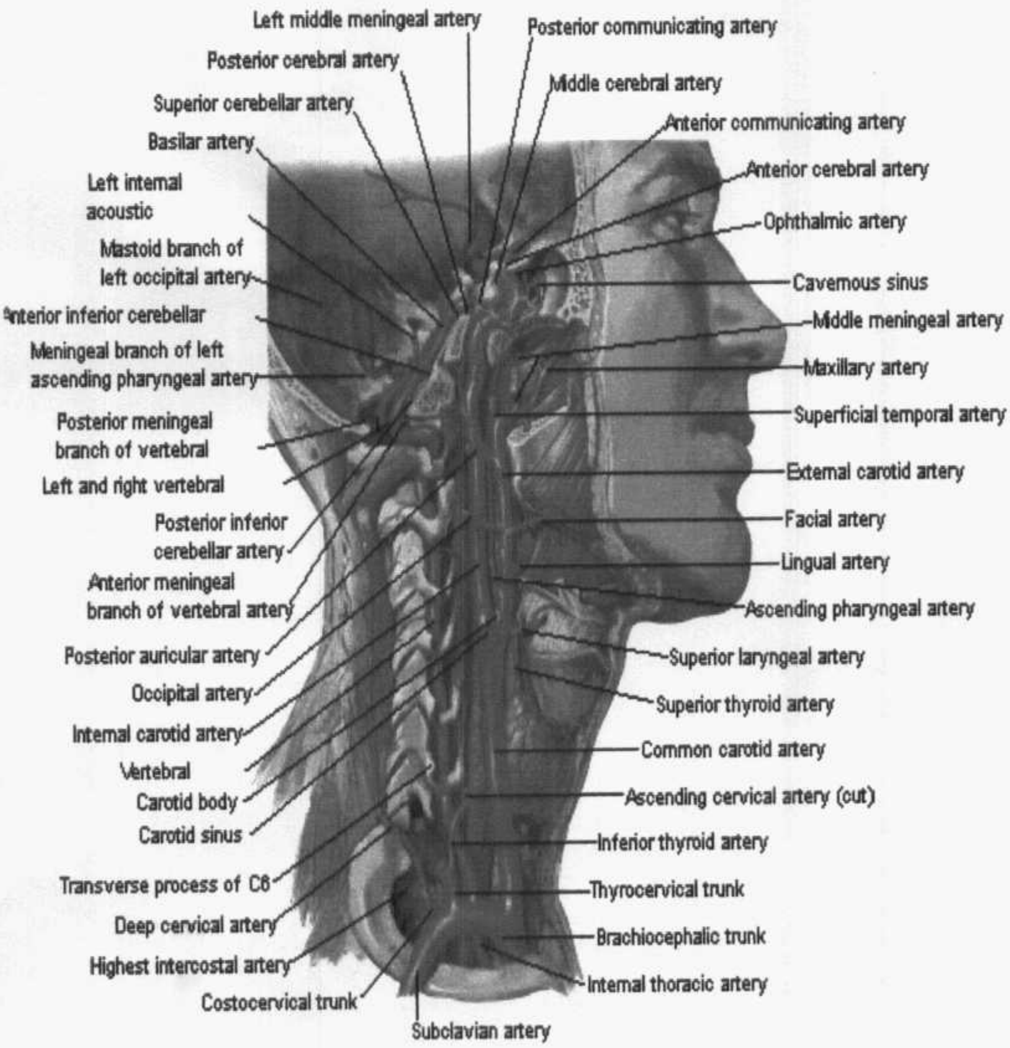

Figure (4): Carotid and vertebrobasilar system
Quoted from (William et al., 1995)

www.manaraa.com

Other parts are:

- Petrous part.
- Cavernous part.
- Cerebral part.**(Williams et at., 1995).**

In the vast majority of patients, the proximal internal carotid is located posterior and lateral to the external carotid. This is very useful feature in distinguishing these two vessels. On occasion, this relationship between the internal and external carotid arteries is reversed. **(Taylor et al., 1987).**

Branches

The cervical part has no branches. Those from the other parts are:

From petrous part:-

- Caroticotympanic
- Pterygoid

From cavernous part:-

- Cavernous
- Hypophyseal
- Meningeal

From cerebral part

- Ophthalmic
- Anterior cerebral
- Middle cerebral
- Posterior communicating
- Anterior choroid **(Williams et al., 1995).**

رات
:om

Pathology of carotid artery diseases

The normal artery:

The general architecture and cellular composition of the blood vessels are the same through the cardiovascular system. However, certain features of the vasculature vary with and reflect distinct functional requirements at different locations. To withstand the pulsatile flow and higher blood pressure in arteries, arterial walls are generally thicker than the walls of veins. Arterial wall thickness gradually diminishes as the vessels become smaller, but the ratio of the wall thickness to lumen diameter becomes greater **(Vinay Kumar et al., 2005).**

The basic constituents of the walls of blood vessels are endothelial cells and smooth muscle cells, and extra cellular matrix (ECM), including elastin, collagen, glycosoaminoglycans. The three concentric layers *intima, media*, and *adventitia* are most clearly defined in the larger vessels, particularly arteries. In normal arteries, the *intima* consists of a single layer of endothelial cells with minimal under lining subendothelial connective tissue. It is separated from the media by a dense elastic membrane called the internal elastic lamina. The smooth muscle cell layer of the media near the vessel lumen receives oxygen and nutrient by direct diffusion from the vessel lumen, facilitated by holes in the internal elastic membrane. However, the diffusion from the lumen is inadequate for the outer portion of the media in large and medium-sized vessels, therefore these areas are nourished by small arterioles arising from outside the vessel (called vasa vasorum) coursing into the outer one half to two thirds of the media. The outer limit of the media of the most arteries is a well-defined external elastic lamina. External to the media is the *adventitia*, consisting of connective tissue with nerve fibers and vasa vasorum **(Vinay Kumar et al., 2005).**

Based on their size and structural features, arteries are divided into three types: **(1)** large or elastic arteries, including the aorta, its large branches (particularly the innominate, subclavian, common carotid, and iliac), and pulmonary arteries; **(2)** medium-sized or muscular arteries, comprising other branches of the aorta (e.g., coronary and renal arteries); **(3)** small arteries within tissues and organs (**Vinay Kumar et al., 2005).**

Arteriosclerosis

Arteriosclerosis is generic term of thickening or loss of elasticity of arterial wall. Three patterns of arteriosclerosis are recognized; they vary in pathophysiology and clinical and pathological consequences.

رات
:om

- *Atherosclerosis*, the most frequent and important pattern will be discussed first and in detail below.

- *Dominant pattern*, characterized by formation of intimal fibrous plaques.

- *Monckeberg medial calcific sclerosis*, is characterized by calcific deposits in muscular arteries in person older than age 50. The radiographically visible, often palpable calcification, do not encroach on vessel lumen.

Arteriolosclerosis affects small arteries and arterioles. There are two anatomic variant, hyaline and hyperplastic, both associated with thickening of vessel walls with luminal narrowing that may cause down stream ischemic injury. Most often associated with hypertension and diabetes mellitus. **(Vinay Kumar et al., 2005).**

The lesion of atherosclerosis occurs primarily within the tunica intima (innermost layer) and includes the fatty streak, fibrous plaque, and advanced or complicated lesion. The fatty streak, the earliest atherosclerotic lesion, is a flat, yellow, lipid filled smooth muscle cell that causes no obstruction of the affected vessel **(Cortran et al., 1999).**

Fibrous plaque is the characteristic lesion of advanced atherosclerosis and is rarely found in people younger than 25

رات
:om

years age. It consists of lipid-laden smooth muscle cell surrounded by collagen, elastic fibers, and a mucoprotein matrix. The lesion is white and elevated and protruded into the lumen of artery. If the lesion progress sufficiently, it can occlude the arterial lumen. This is the most likely to occur at arterial bifurcation, curves or regions in which arteries taper **(Kathryn and Sue, 1994)**.

Complicated or advanced lesion of atherosclerosis is at risk for the following pathological changes that have clinical significance:

- Focal *rupture*, *ulceration*, or *erosion* of the luminal surface of atheromatous plaques
- *Hemorrhage* into plaque.
- Superimposed *thrombosis*, usually occur on disrupted lesions and may partially or completely occlude the lumen.
- *Aneurysmal dilatation* may result from atrophy of underlying media, with loss of elastic tissue, causing weakness and potential rupture. **(Vinay Kumar et al., 2005).**

Risk Factors

1-Hypercholesterolaemia

Is the major risk factor, associated with the increased incidence of atherosclerosis. Although many lesions of

رات
:om

atherosclerosis are fibrous and contain relatively little lipid, the deposition of the lipids on endothelium, on monocytes and on smooth muscle, and the accumulation of lipid in the lesion of hypercholesterolaemic individuals, can be critical components of the process of atherogenesis **(James et al.,1992).**

2-Hypertention

Has long been recognized as a risk factor associated with increase incidence of coronary heart disease, cerebrovascular diseases and accelerated atherogenesis. Epidemiologically, the effects of hypertension appear to be unrelated to those of other risk factors such as hypercholesterolemia, there appear to be a synergetic effect of these in increasing the incidence of atherosclerosis (**James et al., 1992).**

3-Cigarette smoking

Is perhaps one of the strongest epidemiological associations with increase incidence of atherosclerosis. A series of tobacco glycoproteins has been isolated which is said to be associated with an immune response with the arterial wall (**James et al., 1992).**

4- Diabetes mellitus

Is another important risk factor for increase incidence of atherosclerosis. Individuals who have clinical diabetes mellitus

رات
:om

have increase incidence of atherosclerosis and myocardial infarction. Many diabetic individuals are hypercholesterolaemic. However, for those who are norm-cholesterolaemic, the mechanism by which diabetes results in increase lesions of atherosclerosis is poorly understood (**James et al., 1992).**

Carotid atherosclerosis

The majority of thrombotic occlusion is due to atherosclerosis. The most common site of involvement is the carotid bifurcation. Evolution of arterial stenosis varies from progressive narrowing of the lumen and thrombosis which may be accompanied by antegrade extension, to fragmentation and distal embolization **(Umberto et al., 1999).**

The degree was expressed according to NASCET study, the diameter of the residual lumen at the narrowest point of stenosis as related to the diameter of the internal carotid artery (ICA) well beyond the bulb was classified as mild (0-29), moderate (30-69), severe (70- 99) stenosis and occlusions (**North American Symptomatic Carotid Endarterectomy Trial collaborators, 1991).**

Carotid atherosclerosis characterized by intimal lesions called atheromas or fibrofatty plaques that protrude into the lumen, weakening the underlying media and undergoes serious complication. Atheromas are focal and sparsely distributed at first but as the disease advances, they become more numerous and sometimes covering the entire circumference of severely affected arteries. Atheromas may be destructive, encroaching upon the subjacent media and weakening the affected vessel wall causing aneurysms or rupture or favoring thrombosis. In addition, extensive atheromas are friable, often yielding emboli into distal circulation **(Umberto et al., 1999).**

The typical patient of occlusive atherosclerosis disease of carotid artery presents with a history of transient ischaemic attacks together with angina or evidence of coronary artery disease **(Cuschieri et al., 1995).**

Pathogenesis

Understandably, the overwhelming importance of atherosclerosis historically, two hypotheses for atherogenesis were dominant: One emphasized cellular proliferation in the intima, whereas the other emphasized organization and repetitive growth of thrombi. The contemporary view of pathogenesis of atherosclerosis incorporates elements of both older theories and accommodates the risk factor. This concept, called the response to injury hypothesis, considered atherosclerosis chronic inflammatory response of arterial wall

رات
:om

initiated by injury to the endothelium. Moreover, lesion progression is sustained by interaction between modified lipoproteins, monocyte-derived macrophages, T lymphocytes, and normal cellular constituents of arterial wall. **Center to this hypothesis are the following:**

- *Chronic endothelial injury*, usually subtle, with resultant endothelial dysfunction.
- *Accumulation of lipoproteins,* mainly LDL, with its high cholesterol content, in the vessels wall.
- *Modification* of lesional lipoproteins by oxidation
- *Adhesion of blood monocytes* (and other leukocytes) to the endothelium, followed by their migration to the intima and their transformation into microphages and foam cells.
- *Adhesion of platelets*
- *Release of factors* from activated platelets, macrophages, or vascular cells
- *Proliferation* of smooth muscle cells in the intima
- *Enhanced accumulation of lipid* both within cell and extracellular (**Vinay kumer et al., 2005).**

رات

:om

Complication of atherosclerosis and effect of atheromas

Gradual obstruction:

This is most important in coronary and cerebral vessels. Often, no appreciable effect is noted until the lumen is reduced by 70% **(Walter and Talbot, 1995).**

Sudden complete obstruction:

This may either be due to thrombosis or hemorrhage into the plaque. Rupture of the vasa vasorum in the degenerated center region of the plaque will lead to haematoma formation. This may completely block the vessel, and is thought by some authors to be an important factor in acute occlusion **(Walter and Talbot, 1995).**

Dilatation and aneurysm formation:

An aneurysm is a localized abnormal dilatation of blood vessel caused by congenital or acquired weakness in the media. Atherosclerotic aneurysm are usually fusiform in shape (ovoid swelling parallel to the long axis of the vessel), although the saccular variety which is bubble like out pouching of the arterial wall at the site of weakened media may be encountered **(Walter and Talbot, 1995).**

رات
:om

Carotid aneurysm is the third after aortic and lower limb. It occurs mainly in atheromas uncomplicated by thrombotic episodes due to atrophy of the media **(Walter and Talbot, 1995).**

Embolism

An embolus is an abnormal mass of undissolved material that is transported from one part to another. Atheromatous and thrombotic material from the aorta and its major branches sometimes becomes detached and embolises distally **(Walter and Talbot, 1995).**

Carotid Aneurysms

Abnormal dilatations of arteries are called aneurysms. They develop wherever there is marked weakening of the wall of the vessels. Any vessels may be affected by wide variety of disorders that weaken arterial wall, including congenital defect, local infection (mycotic aneurysm) trauma or systemic diseases. Much has been made in the past in the terms saccular, fusiform, cylindriod, berry-shaped in relation to gross appearance of an aneurysm. However, these shapes are not specific for any disease or clinical manifestation (**Kuehne et al., 1996**).

رات

:om

Carotid pseudoaneurysm

Carotid pseudoaneurysms, commonly referred to false aneurysms, are caused by partial or complete disruption of the vessels wall resulting in preluminal hemorrhage contained by surrounding soft tissue. Pseudoaneurysms are common caused by penetrating injuries to the neck and account for 33% to the lesions to the internal carotid artery (**Kuehne et al., 1996).**

Arteriovenous fistula

It is rare, usually small, abnormal communication between arteries and veins. It arises as developmental defect, but can also be produced from rupture of an arterial aneurysm into adjacent vein, from penetrating injuries that pierce the wall of artery and vein, or from inflammatory necrosis of adjacent vessels. Arteriovenous fistula may be of clinical significance because they short-circuit blood from arterial to venous side, thereby causing the heart to pump additional volume; sometimes high output cardiac failure ensues. Moreover, they can rupture and causing hemorrhage, especially in the brain. In contrast, intentionally created arteriovenous fistulas are used to provide vascular access for chronic hemodialysis (**Vinay Kumer et al., 2005).**

رات
:om

Carotid Dissection

Dissection almost always originates with intimal tears. The tear is usually longitudinal or oblique. Blood entering this defect usually penetrates into the media and propagates in the medial laminar planes forming a haematoma. In some instances, haematoma is confined to one arc of the circumference sparing a portion. Sometimes the inner layer may collapse on themselves causing significant vascular obstruction. Dissection is rare in penetrating trauma occurring in fewer than 2%of patients. Most plane traumatic dissection results from hyperextension, rotation or hyperflexion **(Walter and Talbot, 1995).**

رات
:om

EVOLUTION OF COMPUTED TOMOGRAPHY

Since its introduction in 1972, x-ray computed tomography (CT) has evolved into an essential diagnostic imaging tool for a continually increasing variety of clinical applications. Dramatic improvements in image quality, acquisition speed, and patient throughput have resulted from recent technical developments in helical and, more recently, multiple-row detector technologies. This evolution of CT technology is a logical extension of conventional radiography and can be viewed as a progression toward optimizing the information (**Mahadevappa M., 2002).**

CT is fundamentally a method for acquiring and reconstructing an image of a thin cross section of an object. It differs from conventional projection in two significant ways: First, CT forms a cross-sectional image, eliminating the superimposition of structures that occurs in plane film imaging because of compression of 3D body structures into the two-dimensional recording system. Second, the sensitivity of CT to subtle differences in x-ray attenuation is at least a factor of 10 higher than normally achieved by screen-film recording systems

رات

:om

because of the virtual elimination of scatter. (**Mahadevappa M., 2002**).

Historical Developments

CT Generations

First-Generation CT Scanners

The first commercial scanner invented by Hounsfield, was introduced in 1973. This scanner acquired data with an x-ray beam collimated to a narrow "pencil" beam directed to a single detector on the other side of the patient; the detector and the beam were aligned in a scanning frame. A single projection was acquired by moving the tube and detector in a straight-line motion (translation) on opposite sides of the patient (Fig. 5).

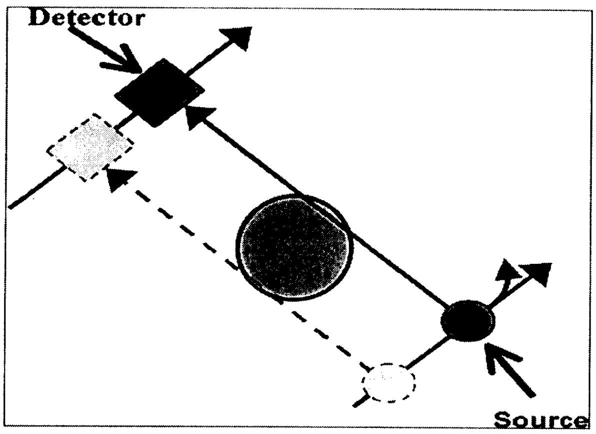

Figure(5): Diagram of first-generation CT scanner, which used a parallel x-ray beam with translate-rotate motion to acquire data (Quoted from Mahadevappa M., 2002).

To acquire the next projection, the frame rotated 1°, then translated in the other direction. This process of translation and rotation was repeated until 180 projections were obtained. The earliest versions required about 4.5 minutes for a single scan and thus were restricted to regions where patient motion could be controlled (the head). Since procedures consisted of a series of scans, procedure time was reduced somewhat by using two detectors so that two parallel sections were acquired in one scan. Although the contrast resolution of internal structures was unprecedented, images had poor spatial resolution **(Hendee WR et al., 1992).**

Second-Generation CT Scanners

The main impetus for improvement was in reducing scan time ultimately to the point that regions in the trunk could be imaged. By adding detectors angularly displaced, several projections could be obtained in a single translation. For example, one early design used three detectors each displaced by 1°. Since each detector viewed the x-ray tube at a different angle, a single translation produced three projections. Hence, the system could rotate 3° to the next projection rather than 1° and had to make only 60 translations instead of 180 to acquire a complete section (Fig. 6).

رات
:om

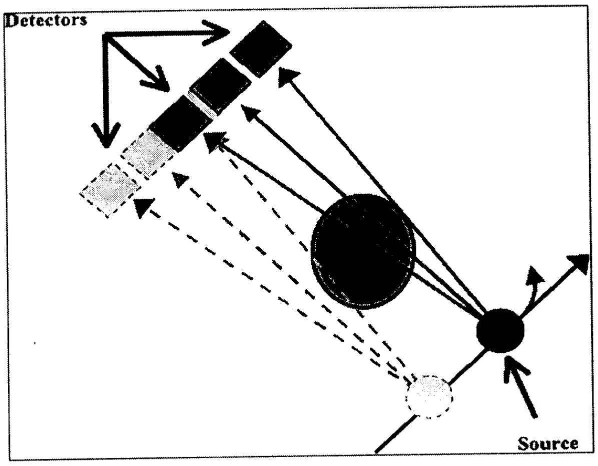

Figure (6): Diagram of second-generation CT scanner, which used translate-rotate motion to acquire data (Quoted from Mahadevappa M., 2002).

Scan times were reduced by a factor of three. Designs of this type had up to 53 detectors, were ultimately fast enough (tens of seconds) to permit acquisition during a single breath hold, and thus were the first designs to permit scans of the trunk of the body. Because rotating anode tubes could not withstand the wear and tear of rotate-translate motion, this early design required a relatively low output stationary anode x-ray tube. The power limits of stationary anodes for efficient heat dissipation were improved somewhat with the use of asymmetrical focal spots (smaller in the scan plane than in the z-axis direction), but this resulted in higher radiation doses due to poor beam restriction to the scan plane. Nevertheless, these scanners required slower scan speeds to obtain adequate x-ray flux at the

رات
:om

detectors when scanning thicker patients or body parts. **(Bushburg JT et al., 1993)**

Third-Generation CT Scanners

Designers realized that if a pure rotational scanning motion could be used, then it would be possible to use higher-power rotating anode x-ray tubes and thus improves scan speeds in thicker body parts. One of the first designs to do so was the so-called third generation or rotate-rotate geometry. In these scanners, the x-ray tube is collimated to a wide, fan-shaped x-ray beam and directed toward an arc-shaped row of detectors. During scanning, the tube and detector array rotate around the patient and different projections are obtained during rotation by pulsing the x-ray source or by sampling the detectors at a very high rate (Fig. 7).

رات

:om

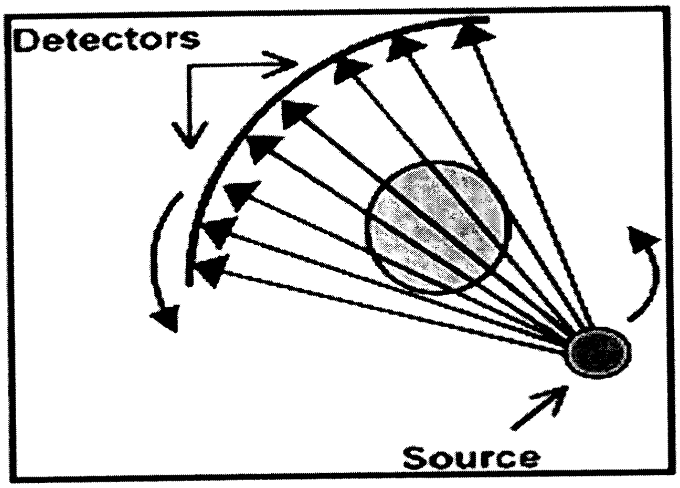

Figure (7) : Diagram of third-generation CT scanner, which acquire data by rotating both x-ray source with a wide fane beam geometry and the detector around the patient. Hence, the geometry is called rotate-rotate motion (Quoted from Mahadevappa M., 2002).

The number of detectors varied from 300 in early versions to over 700 in modern scanners. Since the slam-bang translational motion was replaced with smooth rotational motion, higher-output rotating anode x-ray tubes could be used, greatly reducing scan times. One aspect of this geometry is that rays in a single projection are divergent rather than parallel to each other, as in earlier designs. Beam divergence required some modification of reconstruction algorithms, and sampling considerations required scanning an additional arc of one fan angle beyond 180°, although most scanners rotate 360° for each scan. Nearly all current helical scanners are based on

رات
:om

modifications of rotate-rotate designs. Typical scan times are on the order of a few seconds or less, and recent versions are capable of sub second scan times. .(Bushburg JT et al., 1993).

Fourth-Generation CT Scanners

This design evolved nearly simultaneously with third-generation scanners and also eliminated translate-rotate motion. In this case, only the source rotates within a stationary ring of detectors (Fig.8).

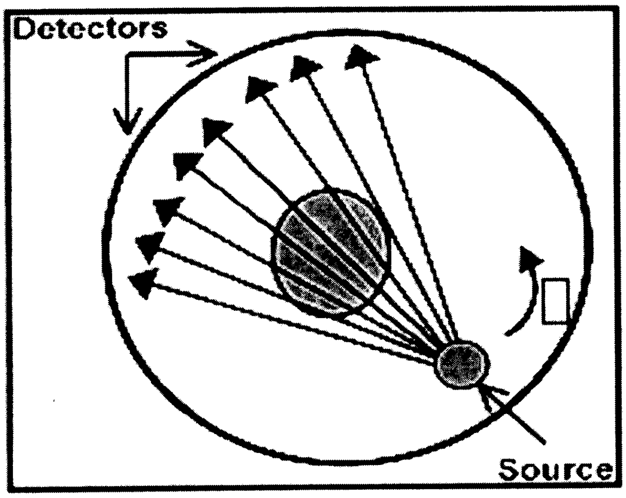

Figure (8): Diagram of fourth-generation scanner, which uses a stationary ring of detectors positioned around the patient. Only the x-ray source rotates with wide fane beam geometry, while the detectors are stationary. Hence, the geometry called rotate-stationary motion (Quoted from Mahadevappa M., 2002).

:om

The x-ray tube is positioned to rotate around the patient within the space between the patient and the detector ring. One clever version, which is no longer produced, moved the x-ray tube out of the detector ring and tilted the ring out of the x-ray beam in a wobbling motion as the tube rotated. This design permitted a smaller detector ring with fewer detectors for a similar level of performance. Early fourth-generation scanners had some 600 detectors and later versions had up to 4,800. Within the same period, scan times of fourth-generation designs were comparable with those of third-generation scanners. One limitation of fourth-generation designs is less efficient use of detectors, since less than one-fourth are used at any point during scanning. These scanners are also more susceptible to scatter artifacts than third-generation types, since they cannot use antiscatter collimators. CT scanners of this design are no longer commercially available except for special-purpose applications. **(Mahadevappa M., 2002).**

Principles of Helical CT Scanners:

The development of helical or spiral CT around 1990 was a truly revolutionary advancement in CT scanning that finally allowed true 3D image acquisition within a single breath hold. The technique involves the continuous acquisition of projection data through a 3D volume of tissue by continuous rotation of the x-ray tube and detectors and simultaneous translation of the patient through the gantry opening. (Fig.9)

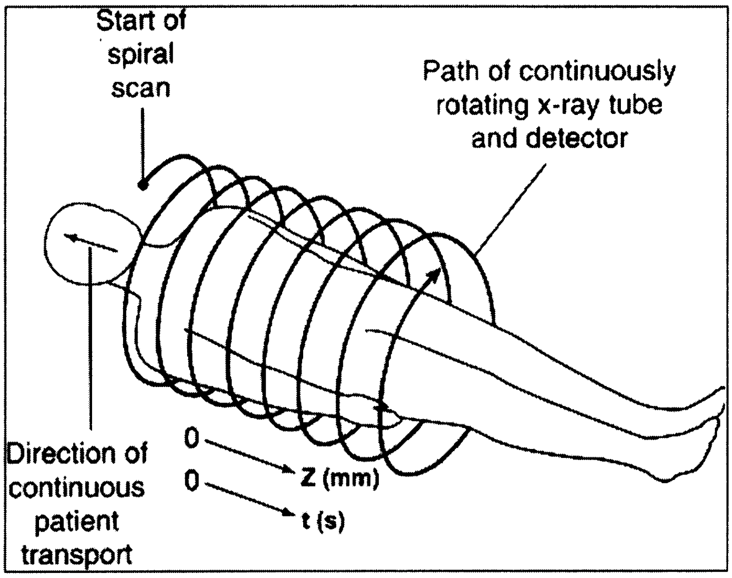

Figure (9): Principle of helical CT. as the patient is transported through the gantry, the x-ray tube trace a spiral or helical path around the patient (Quoted from Mahadevappa M., 2002).

Three technological developments were required: slip-ring gantry designs, very high power x-ray tubes, and interpolation algorithms to handle the non-coplanar projection data. (**Beck TJ., 1996).**

:om

Slip-Ring Technology

Slip rings are electromechanical devices consisting of circular electrical conductive rings and brushes that transmit electrical energy across a moving interface. All power and control signals from the stationary parts of the scanner system are communicated to the rotating frame through the slip ring. The slip-ring design consists of sets of parallel conductive rings concentric to the gantry axis that connect to the tube, detectors, and control circuits by sliding contactors (Fig.10).

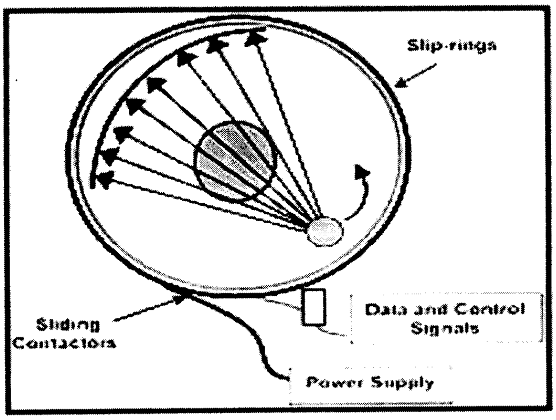

Figure (10): Diagram of slip-ring configuration (Quoted from Brunnett CJ et al., 1994).

:om

These sliding contactors allow the scan frame to rotate continuously with no need to stop between rotations to rewind system cables .This engineering advancement resulted initially from a desire to reduce interscan delay and improve throughput. However, reduced interscan delay increased the thermal demands on the x-ray tube; hence, tubes with much higher thermal capacities were required to withstand continuous operation over multiple rotations. **(Brunnett CJ et al., 1994).**

High-Power X-ray Tubes

X-ray tubes are subjected to far higher thermal loads in CT than in any other diagnostic x-ray application. In early CT scanners, such as in first- and second-generation, stationary anode x-ray tubes were used, since the long scan times meant that the instantaneous power level was low. Long scan times also allowed heat dissipation. Shorter scan times in later versions of CT scanners required high-power x-ray tubes and use of oil-cooled rotating anodes for efficient thermal dissipation. Heat storage capacities varied from 1 million to 3 million heat units in early third-generation CT scanners. The introduction of helical with CT continuous scanner rotation placed new demands on x-ray tubes.

رات
:om

Several technical advances in component design have been made to achieve these power levels and deal with the problems of target temperature, heat storage, and heat dissipation. For example, the tube envelope, cathode assembly, and anode assemblies including anode rotation and target design have been redesigned. (As scan times have decreased, anode heat capacities have increased by as much as a factor of five, preventing the need for cooling delays during most clinical procedures, and tubes with capacities of 5–8 million heat units are available. In addition, improvement in the heat dissipation rate (kilo–heat units per minute) has increased the heat storage capacity of modern x-ray tubes. The large heat capacities are achieved with thick graphite backing of target disks, anode diameters of 200 mm or more, improved high-temperature rotor bearings, and metal housings with ceramic insulators, among other factors. The working life of tubes used to date ranges from 10,000 to 40,000 hours, compared with the 1,000 hours typical of conventional CT tubes. Because many of the engineering changes increased the mass of the tube, much of the design effort was also dedicated to reducing the mass to better withstand increasing gantry rotational rates required by ever faster scan times. **(Fox SH., 1995)**

رات
:om

Capabilities of Single-Row Detector Helical CT

With the advent of helical CT, considerable progress was made on the road toward 3D radiography. Complete organs could be scanned in about 30–40 seconds. Artifacts due to patient motion and tissue misregistration due to involuntary motion were virtually eliminated. It became possible to generate sections in any arbitrary plane through the scanned volume **(Fishman EK et al., 1991**).

Significant improvements in z-axis resolution were achieved due to improved sampling, since sections could be reconstructed at fine intervals less than the section width along the z axis. Near-isotropic resolution could be obtained with the thinnest (-1 mm) section widths at a pitch of 1, but this could be done only over relatively short lengths due to tube and breath-hold limitations.**(Kalender WA., 1995).**

Higher-power tubes capable of longer continuous operation coupled with faster rotation speeds could scan greater lengths with higher resolution. The practical limit on such brute force approaches, however, became the length of time a sick patient could reliably suspend breathing. This turns out to be no more than 30 seconds. Even though the z-axis resolution for helical CT images far exceeds that of conventional CT images, the type of interpolation algorithm and the pitch still affect the

رات
:om

overall image quality. The section sensitivity profiles of helical CT images are different compared with those of conventional CT images, which are influenced by the type of interpolation algorithm and the selected pitch **(Levy RA., 1995).**

Multiple-Row Detector Helical CT

Continued scanner development on the road to a 3D radiograph called for further progress, but single-row detector helical scanners had reached their limits. An obvious improvement would be to make more efficient use of the x rays that are produced by the tube while improving z-axis spatial resolution; this led to the development of multiple-row detector arrays. The principal difference between single- and multiple-row detector helical scanners is illustrated in (Fig.11).

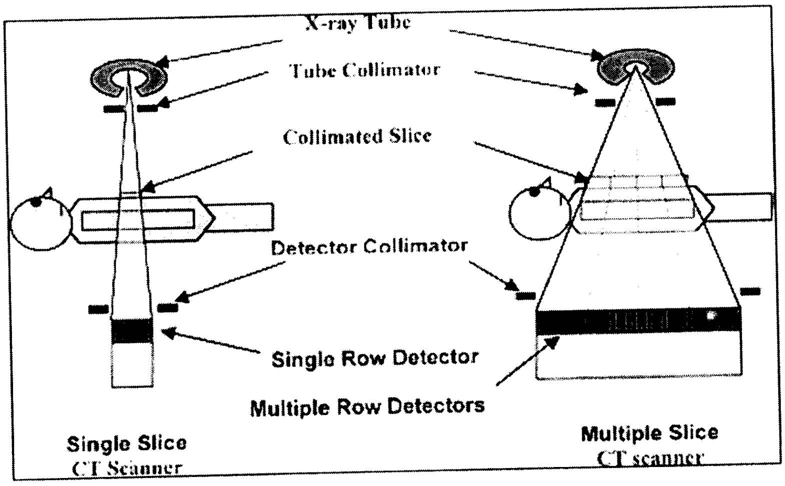

Figure (11): Diagram shows the difference between single-row detector and multiple-row detector CT designs (Quoted from Foley WD et al., 2000).

The basic idea actually dates to the very first EMI Mark I scanner, which had two parallel detectors and acquired two sections simultaneously. The first helical scanner to use this idea, the CT Twin (Elscint, Haifa, Israel), was launched in 1992. This design was so superior to single-row detector designs that all scanner manufacturers went back to the drawing board. By late 1998, all major CT manufacturers launched multiple-row detector CT scanners capable of acquiring at least four sections per rotation. The arrangement of detectors along the z axis and the widths of the available sections vary between the systems. (Fig.12) (**Foley WD et al., 2000).**

In single-row detector helical CT designs, scan volume can be increased with an increased pitch at the expense of poorer z-axis resolution, whereas z-axis resolution can be preserved in multiple-row detector designs. For example, if a 10-mm collimation were divided into four 2.5-mm detectors, the same scan length could be obtained in the same time but with a z-axis resolution improved from 10 mm to 2.5 mm. In another example, a multiple-row detector scanner with four 5-mm detectors and a beam width of 20 mm reduces the scan times for the same z-axis resolution .By increasing the number of CT scanner detector rows, data acquisition capability dramatically increases while greatly improving the efficiency of x-ray tubes. Further developments in scanner rotational speeds and tube

رات

:om

outputs have made isotropic resolution a practical possibility with even better improvements on the horizon. Current multiple-row detector scanners can scan large 40-cm volume lengths in less than 30 seconds with near-isotropic resolution and image quality (**Foley WD et al., 2000**).

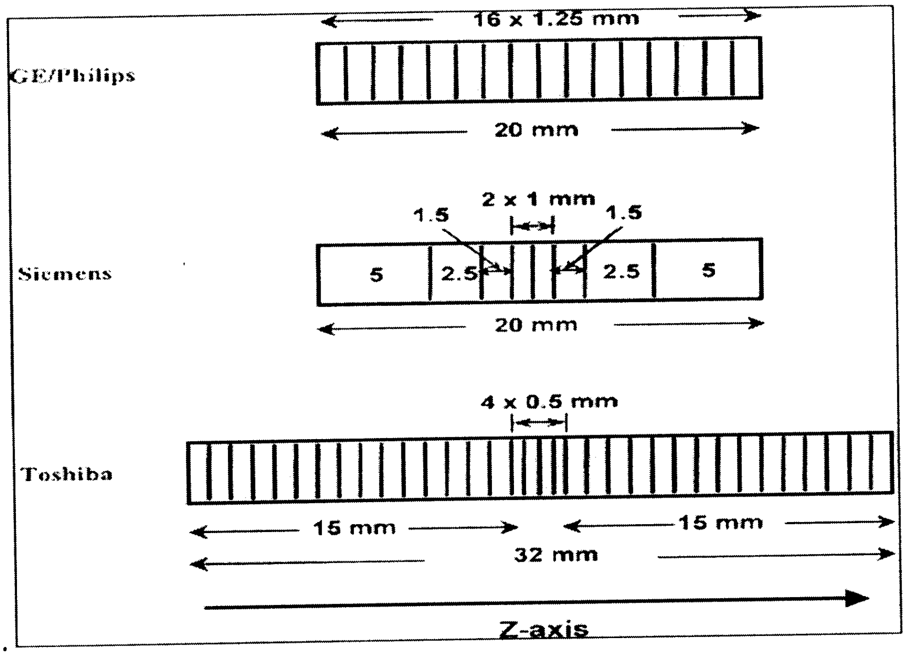

Figure (12): Various detectors array designs used in multiple-row detector CT scanners (Quoted from Foley WD et al., 2000).

Helical Pitch

With single-row detector helical CT scanners, the concept of pitch is straightforward. With the beam width given by W (in millimeters) and the table travel per gantry rotation defined as T

(in millimeters), pitch and more specifically the *beam pitch* is defined as follows (Fig. 13)

With the introduction of multiple-row detector CT scanners, ambiguity arises in terms of the definition of pitch, since different manufacturers use different definitions of pitch, which has resulted in much confusion.

Consequently, beam pitch needs to be distinguished from *detector pitch*, which is defined as follows:

Detector pitch= T/D

where D is the detector width in millimeters (Fig.13).

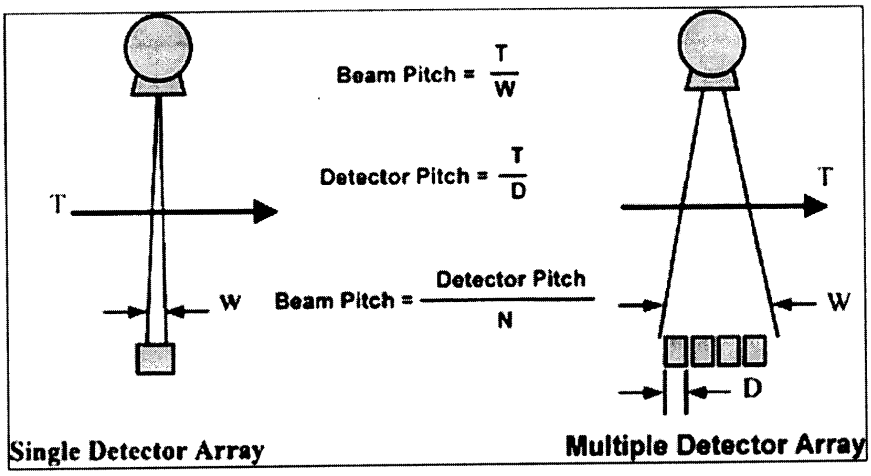

Figure (13):Diagram shows the concepts of beam pitch detector pitch. D=detector width, N=number of active detectors, T=table travel per gantry rotation, W=beam width (Quoted from Silverman PM et al., 2001).

If the x-ray beam is collimated to *N* active detectors in a multiple-row detector CT scanner, the relationship between beam pitch and collimator pitch is as follows:

Beam pitch=Detector pitch/N

Beam pitch = T / D x N **(Silverman PM et al., 2001).**

The use of beam pitch is applicable equally to both single-row detector helical CT and multiple-row detector CT and eliminates the confusion existing between the relationship of radiation dose and various manufacturers defined pitch (**Mahesh M et al., 2001)**.

Advantages of Multiple-Row Detector CT

The clinical advantages of multiple-row detector technology can be broadly divided into two categories: (*a*) Its speed can be used for fast imaging of large volumes of tissue with wide sections. This is particularly useful in studies where patient motion is a limiting factor. With a four-section system and a 0.5-second rotation, the volume data can be acquired eight times faster than with a single-row detector, 1-second scanner. (*b*) The other main advantage of multiple-row detector systems is their ability to cover large volumes in short scan times. The volume coverage and speed performance in a multiple-row detector CT scanner are better than in its counterpart single-row

رات

:om

detector helical CT scanner without compromises in image quality.

One of the most important promises of multiple-row detector technology is that of true isotropic spatial resolution, that is, cubic voxels, so that the image is equally sharp in any plane traversing the scanned volume. This capability is reasonably achieved with multiple sections of 1-mm thickness or less. Ideally, the true 3D radiograph would have cubic voxels of less than 1 mm acquired over large volumes with very short times, at least within a reasonable breath hold. CT angiography, which was possible with the single-row detector helical scanners, became practical with multiple-row detector scanners. The fast rotation times and large volume coverage provide improved multiplanar reconstruction and 3D images (Fig.14) with reduced image artifacts **(Lawler LP et al., 2001).**

This technology also opens up new possibilities for applications in trauma, geriatric, and pediatric examinations. Improved accuracy in 3D volume coverage has led to the development of CT fluoroscopy and CT virtual endoscopy (**Fishman E.K et al., 2001**).

رات
:om

Figure (14):three-dimensional image reconstructed from Multiple-row detector helical CT data (Quoted from Lawler LP et al., 2001).

Detectors rows and array design

Type of detectors

The multiple detector arrays are an assembly of multiple solid-state detectors array modules which is composed of a scintillator coupled tightly to a photodetector. The scintillator emits visible light when it is strucked by X-rays intensifying screen. The light emitted by the scintillator reaches the photodetector, which is an electronic device that converts light intensity into an electrical signal proportional to light intensity. The scintillator used in solid-state CT detectors varies among manufacturers, with $CdWO_4$, yttrium and gadolinium cermics and other material being used **(Jerrold et al., 2002).**

www.manaraa.com

Detector rows:

A single-slice helical CT scanner has one x-ray tube and a single row of detectors this detector row contains 500-900 detector elements, which describe an arc in transverse (axial or x-y) plane, providing one channel of spatial data. Multislice CT (MSCT) scanner has one x-ray tube and multiple rows of detectors along (z) axis of the patient. Each row has 500-900 elements, and many rows together create a two-dimensional curved array containing thousand of detector elements, which are connected to multi data acquisition systems that generate more than one channel per gantry rotation (**Rydberg et al., 2000**).

A single-slice helical scanner has a data acquisition system (DAS) that allows registration of only one channel of image information of the scanned body part per gantry rotation. To acquire 48 slices with pitch of 1 the gantry has to rotate 48 times. Such a scan typically requires 48 seconds because single-slice CT gantry rotates one per second.

With MSCT (also called multichannel CT, multidetector row CT, or multisection CT) the single detector is replaced multiple rows of detectors which allow for registration of more than one channel per gantry rotation. If the detector row array is equipped with the capacity to collect four simultaneous channels

رات
:om

of information during each gantry rotation, the scanner is called a four-channel scanner (**Rydberg et al., 2003**).

Comparing with a single slice channel scanner, a four-channel scanner has a four-fold capacity to register slices during gantry rotation. In the previous example the scanned time is reduced from 48 seconds to 12 seconds, if the number of the simultaneous registers channels to 8 or 16 by adding more electronics to the detector system, the capacity to register slices increased similarly **(Rydberg et al., 2003).**

Detector array Design

To register four sections simultaneously, a minimum of four detectors must be placed side by side along the z axis. To offer a choice of several section thicknesses, more than four detectors elements along the z axis are required **(Ryberg et al., 2000).**

Two main detectors designs are available: fixed array detector (equal-width detectors) and adaptative array detector (unequal-width detectors) (Fig.15) **(Thomas G. et al 2005).**

:om

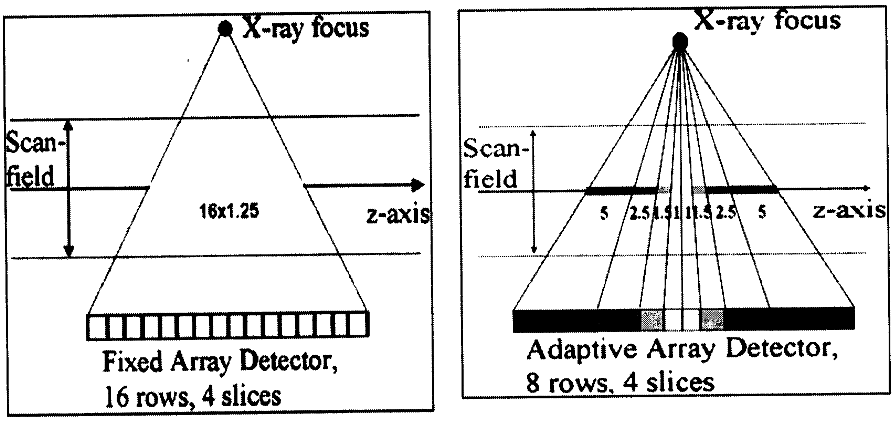

(A) (B)

Figure (15). Illustrations show examples of (A) fixed-array and (B) adaptive-array detectors used in commercially available four- and 16-section CT systems (Quoted from Thomas G. et al., 2005).

For scanning with fixed array detector, the detector array is composed of several small juxtaposed detectors. The GE light speed is composed of 16 rows of 912 1.25mm thick detector elements stacked in the z direction. X-ray beam collimation, selection of the detector row, and coupling of both defines the collimation of the images. It is possible to acquire simultaneous 4 slice of 1.25mm each, 4 slice of 2.5mm (coupling of 2 contiguous rows of detectors along the z direction), 4 slices of 3.75mm (coupling of 3 rows), or 4 slices of 5mm (coupling of 4 rows) **(Blum et al., 2000).**

Selection of slice thickness

The slice thickness in single detector array CT systems is determined by the physical collimation of the incident x-ray beam with two lead jaws. As the gap between the two lead jaws widens, the slice thickness increases. The width of the detectors in single detector array places an upper limit on the slice thickness. Opening the collimation beyond this point would do nothing to increase slice thickness, but would increase both of dose to the patient and amount of scatter radiation **(Jerrold et al., 2002).**

The slice thickness of multiple detectors array CT scanners is determined not by the collimation, but rather by the width of the detectors in the slice thickness dimension **(Jerrold et al., 2002).**

Isotropic imaging

Isotropic viewing refers to the situation in which MPR images can be created in any plane with the same spatial resolution as the original sections. For scanning of small body parts, isotropic viewing is achieved by using the small focal spot on the anode and scanning with ultra thin sections (0.5mm) resulting in a longitudinal resolution nearly identical to the in-plane resolution. Reformatting images (coronal, sagittal, and axial) can be created from one helical acquisition. For example,

رات
:om

in imaging of the temporal bone, the need for direct coronal scanning is avoided because reformation images have the same spatial resolution as the images obtained with direct coronal scanning. The examination can be done faster, with improved patient comfort, and less radiation. More information is derived from MPR images created from one multisection acquisition collimated to 0.5 mm than from two conventional acquisitions (direct axial and direct coronal) collimated to 1mm **(Rydberg et al., 2000).**

Thin-section scanning produces fine in-plane detail and also allows for different types of postprocessing, such as multiplanar reformation (MPR), volume rendering (VR), and surface shaded display (SSD). When the slice thickness approaches the in-plane resolution of the images the term isotropic imaging can be applied. Isotropic imaging implies that voxels that build up the volume data set are cuboidal in shape compared with nonisotropic imaging, where the voxels have a noncuboidal shape. Isotropic imaging minimizes the importance of patient positioning and obviates the need to obtain axial, coronal, and sagittal planes directly. Isotropic imaging also optimizes postprocessing, such as multiplanar reformats, volume rendering, and surface shaded display **(Rydberg et al., 2003).**

رات
:om

Scanning speed and anatomic coverage

The multislice scanners allow for very fast scanning. The high speed allows for one-breathhold scanning with large anatomic coverage. There are fewer motion artifacts in situations when a patient has difficulty lying still. The faster scanning allows for both reductions in intravenous contrast media doses and high injection rate because the scan times are significant reduced. Fast scanning using a multislice scanner also allows for better tube use. With single slice system, tube overheating limits the possibility of scanning long coverage with thin collimation. With wider collimation used with MSCT a higher tube current can be applied because the scanning is done faster. Collimation, pitch, and scanning time divided by gantry rotation time. The following three calculations illustrate the anatomic coverage capability of MSCT scanners. In all three cases it is assumed that the pitch is constant (pitch=1). If scanning is done for 15 seconds with 1-mm collimation on a single-slice scanner (1-second gantry rotation time) the anatomical coverage becomes 15mm. if the same scan time (15seconds) is applied to the 4 x 1 mm mode on a four-slice scanner with 0.5-second rotation time the anatomic coverage become 120mm. if the same calculation is done on a 16-slice scanner using 12-mm collimation and a 0.4-second gantry rotation time the anatomic coverage becomes 423mm. a 16-slice

رات
:om

scanner has approximately 30 times greater coverage capacity than a four-slice scanner when a 1-mm slice thickness on the single-slice system is chosen as the reference (Fig.16) **(Rydber et al.,2003).**

Figure (16): long coverage. MPR of chest, abdomen, and pelvis. MSCT offers long anatomic coverage with high spatial resolution (Quoted from Rydberg et al., 2000).

www.manaraa.com

The increase in scanning speed can be used exclusively to reduce the scanning time, or the faster scanning capability can be exchanged for thinner collimation, yielding higher spatial resolution. Changes in these two parameters are not mutually exclusive. Often, a combination of reduced scanning time and increase spatial resolution is advantageous. The advantages of multislice scanning are as follows:

Improved temporal resolution: Faster scanning results in fewer motion artifacts due to voluntary and involuntary movement (e.g., intestinal peristalsis, respiration). Breathing holding times are reduced **(Blum et al., 2000)**.

Improved spatial resolution in the z axis: Thinner sections improve resolution in the z axis (along the table), reducing partial volume artifacts, and increase diagnostic accuracy (**Mahesh 2002**) **.**

Increase concentration of intravenous contrast material: Because scanning is done more quickly, contrast material can be administrated at a faster rate, improving the appearance of arteries, veins, and pathological conditions rich in blood flow (eg, aneurysms, hypervascular tumors, active bleeding). The separation between arterial and venous phases is improved **(Blum et al., 2000).**

***Decrease image noise*:** Because imaging is completed rapidly, x-ray tube current (mA) may be increased, decrease image noise and improving quality, especially important when using thin slice and/or imaging large patient (**Rydberg et al., 2000**).

***Efficient x-ray tube utilization*:** Because imaging is completed rapidly, x-ray tube heating is diminished, decrease or eliminating the need to wait for tube cooling between scans. More images are produced during the lifetime of the tube and decreasing operating costs **(Rydberg et al., 2000).**

***Longer anatomic coverage*:** A great advantage of multislice CT over single-slice helical CT is the opportunity for longer anatomic coverage. The longer coverage is due to the simultaneous registration of at least four sections during each rotation and increased gantry rotation speed. The coverage can be at least eight times longer than that of single-slice helical CT with the same scanning time **(Mahesh 2002) .**

رات
:om

Radiation dose

Multislice scanners employ the same detector material, and have the same gantry geometry and x-ray beam filtration as their single slice counterparts. The main difference lies in the z-axis geometric efficiency, where irradiated slice width is generally wider than the active detectors width. This is to avoid calibration problems that can occur when the outermost elements of the active array are exposed to the x-ray beam penumbra. Varying claims have been made regarding doses from multislice scanners. An early version of one multislice model resulted in doses, as measured by the computed tomography doses index (CTDI), that were up to three times higher than a single slice model from the same manufacture. This high dose resulted from the extend of the x-ray beam beyond the active detector length and reinforced the view that multislice scanners gives rise to increased doses. On current multislice models however, when widest collimation are employed, the CTDI for a given tube current-exposure time product (mAs) is approximately 10% higher than for single scanners, but because the z-axis geometric efficiency decreases with total x-ray collimation, for 1mm slices the values are about 40% higher than for well collimated single slice systems. The view that multislice systems will result in increased doses is also supported by their ability to perform a wider range of

رات
:om

applications, the possibility of scanning longer volumes and their capability of performing multiphase contrast studies. Conversely, it has been claimed that multislice CT will lead to a reduction in doses levels. In support of this view, it is claimed that the shorter examination time reduce the need for repeat examinations caused by patient movement or incorrectly timed contrast study **(Lewis 2001)**.

رات
:om

Technique of carotid CT angiography

CT angiography was described as a new minimally invasive method for volumetric display of contrast filled vessels.

CT angiography requires the rapid acquisition provided by a spiral CT scanner coupled with an accurately timed high-flow peripheral intravenous injection of iodinated contrast material. The resultant images are processed with computed rendering technique to generate three-dimensional images of the vasculature **(Rubin et al., 1995**).

CTA provides many advantages for imaging the vascular system, including thee-dimensional (3D) volumetric analysis, minimally invasive vascular opacification, and depiction of mural calcium and stent-grafts, and compared with conventional projectional angiography, it provides improved diagnostic accuracy, treatment planning, and lower coasts **(Rubin et al., 2000).**

The technique of CT angiography consists of two steps:

First step is CT angiogram acquisition and second step is CT angiogram pos-processing.

رات

:om

The first step consists of the following:

- Scout view of the part to be examined (Fig. 17).
- Acquisition of a plain localizer group.
- Determination of delay time though test dose injection.
- Finally, Acquisition of CT angiogram.

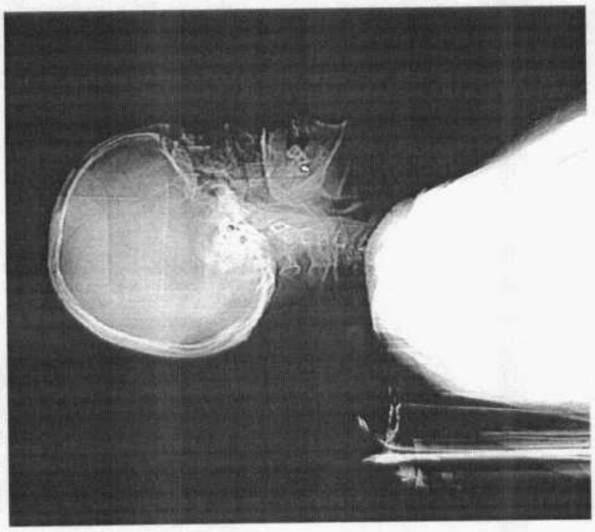

Figure (17): Acquisition of a scout view is the first step in CT angiography Quoted from (Rubin et al., 2000).

The second step of post-processing is divided into:

- Image reconstruction.
- Multi planar and three-dimensional renderings **(Rubin et al., 1995).**

Carotid bifurcation imaging is technically well suited to computed angiography (CTA) because of the large-caliber,

www.manaraa.com

minimal motion and generally longitudinal orientation of these vessels **(Haaga et al., 1994)**.

I-Acquisition of CT angiogram

Acquisition parameters: to acquire a CT angiogram scan length, collimation and table speed, total scan time, reconstruction intervals and plan for contrast media administration should be determined.

A-Scan length:

The carotid bifurcation lies between C2 and C3 in 91% of cases **(Elliot and Brooke, 1998).**

It is determined by performing a low-resolution helical scan using 10 mm collimation and a pitch 2:1. The aim of this scan (localizer group) is to identify the location of the carotid bifurcation and thus defining the cranial and caudal extension of CT angiography **(Robin et al., 1995).**

The scanner is then positioned to start the CT angiography evaluation of the carotid artery 2–3cm below the carotid bifurcation **(Elliot and Brooke , 1998)**.

رات
:om

Usually in carotid CTA, we cover a distance of 6-9 cm. Extended scan range can be done, especially if carotid endarterectomy is planned, using longer exposure time and increase pitch **(Rubin et al, 1995).**

N.B: It is imperative that the patient be coached to obtain the same degree of inspiration during localizing section, otherwise , the anatomy of interest may be shifted out of the imaging volume. Also, patient who can sustain longer breath hold, we can increase the scan coverage or we can use a low pitch thus increasing the resolution **(Rubin et al, 1995).**

B- Slice thickness and table feed:

Slice thickness: as with conventional scanning, choice of slice thickness sitting for helical scanning is based largely on the region of interest and the diagnostic goal of the scan. It is well known that decreasing slice thickness results in increasing resolution and vise versa but on the expense of increasing scan time , X ray dose and amount of contrast media in carotid CTA , slice thickness is sit on 2 mm (**Brink et al .,1995).**

Table speed: increasing table speed without increasing slice thickness (pitch > 1) results in increasing imaged volume and decreasing scan time but unfortunately leads also to decrease in resolution due to increase volume averaging **(Thomas et al., 1995)**

In carotid CTA we use table feet 3mm/sec. (pitch =1.5) **(Brink et al., 1995).**

C-Total scan time:

It depends on scan length and table feed. In carotid computed angiography (CTA), to cover a distance of 9cm with table feed 3mm/sec., total scan time equals 30 seconds **(Brink et al., 1995).**

D-Image reconstruction intervals:

The choice of reconstruction is also critically important in the success of specialized helical CT applications such as CT angiography. After the acquisition of a spiral volume data set, the images can be reconstructed at determined interval along the z-axis. In carotid CTA, the image reconstruction interval is 1mm **(Heiken et al., 1993).**

E-Delay time and plan of contrast media administration:

It is also important to acquire the helical scan for CT angiography during the phase of maximal arterial enhancement with minimization of the parenchyma and venous enhancement.

This is particularly important for generating 3-D rendering that require minimal pre-rendering image editing (Fig.18) **(Galanski et al., 1993).**

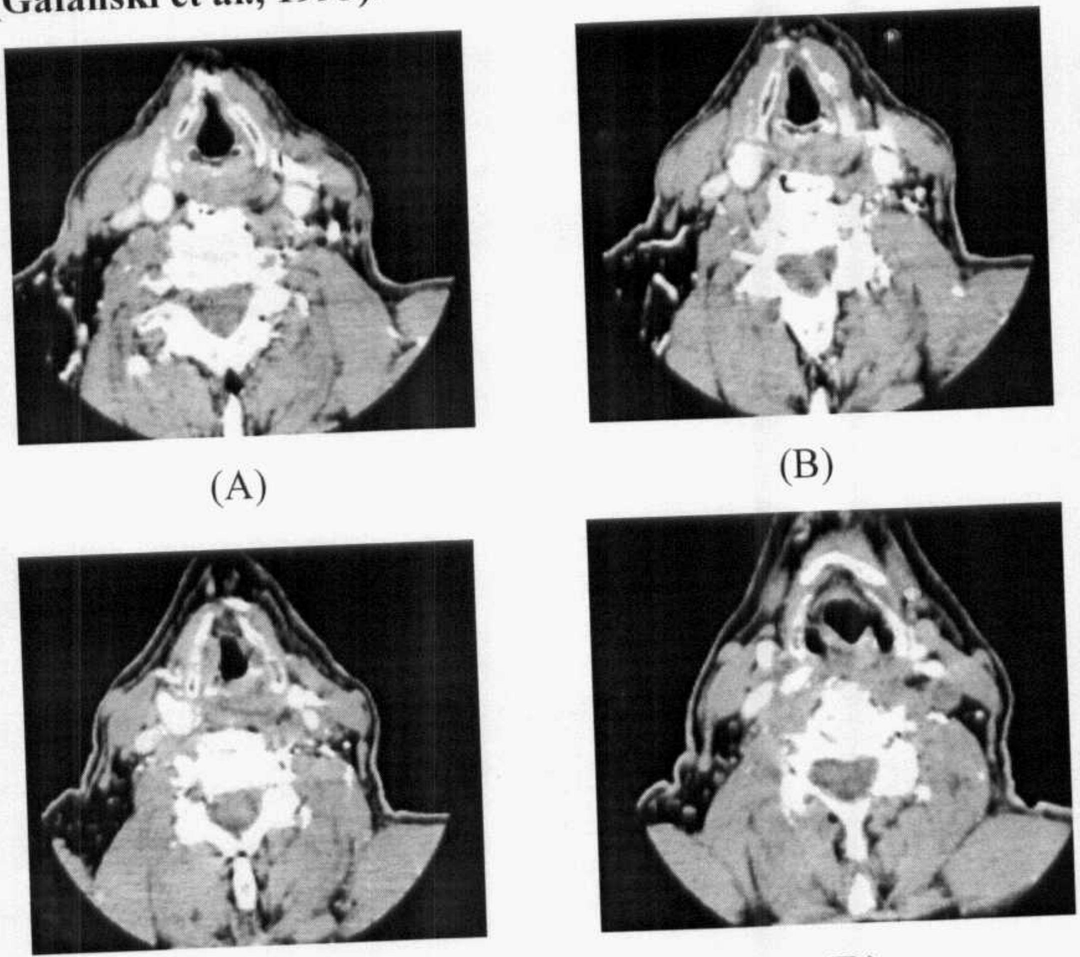

(A) (B)

(C) (D)

Figure (18): axial CT cuts at carotid bifurcation with 1.25 mm interval.. Maximum vascular enhancement is noted. Quoted from (Rubin et al., 2000)

To determine delay time , preliminary bolus injection of 20ml non-ionic contrast is administered over 5 sec (4ml/sec) using 20-gauge ante-cubital vein cannula. Following 8 seconds delay, 12 images (5mm thick) are performed without table

المنارة للاستشارات
www.manaraa.com

movement, these are done at a rate of 2scans/second using 100kvp and 140mas (Fig.19) **(Elliot and Brooke , 1998)**.

Contrast medium administration: (following predetermined delay or by using automatic triggering mechanism):-

- Contrast medium: non-ionic contrast medium
- Amount: 100-120ml.
- Injection rate: 4ml/sec using injector.
- Injection route: 20-gauge RT ante-cubital annula.(RT side is preferred due to haemodynamic and vascular anatmic data) **(Elliot and Brooke , 1998)**.

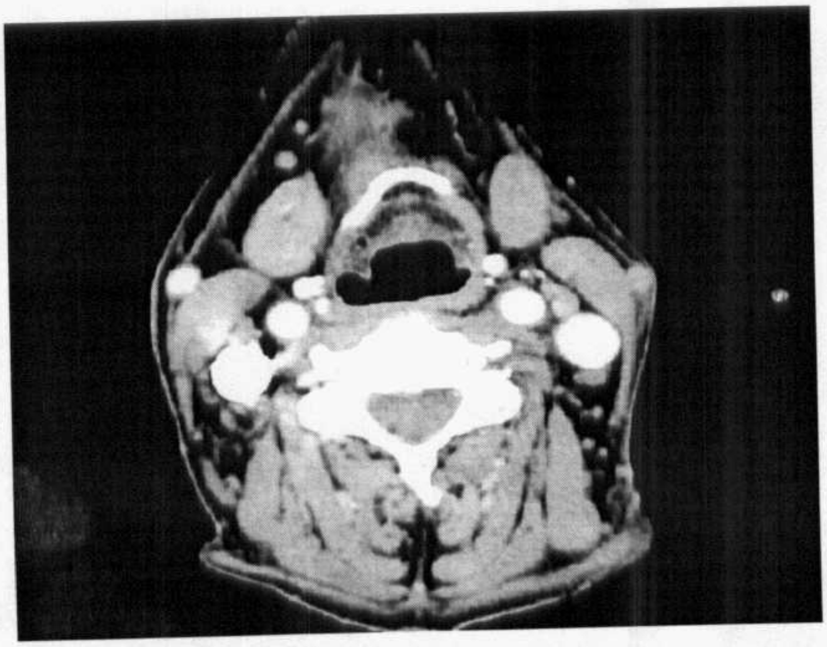

- Figure (19): demonstrating good opacification of vascular structures mandatory for performing CT angiography. Quoted from (Elliot and Brooke, 1998).

المنارة للاستشارات
www.manaraa.com

Important notes:

Other parameters include:

- Field of view = 22cm, map =220, kvp = 120
- Scanning is performed from inferior to superior to follow the direction of the bolus and if possible, a single breath-hold is used to minimize patient motion **(Elliot and Brooke , 1998)**.
- Dual lesion are most frequent at carotid origin and carotid siphon and the detection of these lesions is critical before performing carotid endarterectomy since the patients with such lesions are at greater risk for intra-operative and peri-operative strokes and significant cardiac complications **(Evan et al., 1993).**
- Reducing parenchymal and venous enhancement needs short scan times, which require faster patient translation. But with a fixed gantry rotation period, faster translation reduces the resolution. Recent multi-detector ring scanner and faster gantry rotation, permit faster translation without increasing pitch; that is, without reducing the resolution **(Napel, 1998).**

المنارة للاستشارات
www.manaraa.com

II-CT angiography post-processing

1-Image reconstruction:

Image reconstruction is the first step in CT angiography pos-processing. With image reconstruction, it is possible to produce axial CT images separated by no more than one millimeter if desired (Fig.20). This is performed retrospectively without an increase in x-ray dose that would be present if such images had been generated with conventional scanning (**Brink et al., 1995).**

The value of producing such overlapping images lies in improved small vessels visualization and being able to produce smoother tree-dimensional rendering (**Rubin et al., 1995).**

المنارة للاستشارات
www.manaraa.com

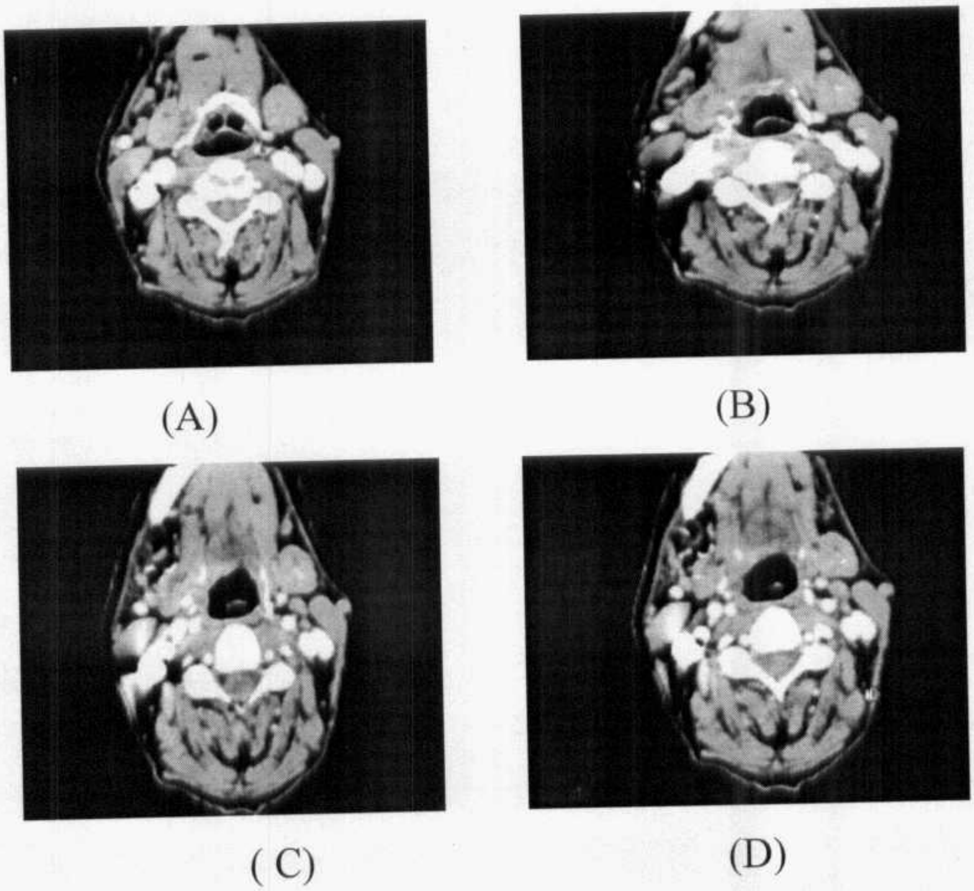

- Figure (20): showing reconstructed axial images at 1mm interval at the level of carotid artery bifurcation (Quoted from Elliot and Brooke, 1998).

2-three dimensional rendering techniques:

The unique advantage of the volumetric spiral CT acquisition is that 3-D rendering can de generated that provides views of the imaging volume from innumerable view angles. Although many of the views can be obtained to simulate various conventional atreriographic projections, additional view angles that are impossible with conventional arteriography are possible with CT angiography.

www.manaraa.com

Four rendering techniques have been used on spiral CT scans: *threshold shaded surface display (SSD), maximum intensity projection (MIP), multi/curved planar reformation and volume rendering (Brink et al., 1995).*

A-Shaded Surface Display:

Any voxel above a certain threshould of density will be displayed; therefore the surface of an object can be displayed. pixels farther from the viewer can be made less bright, giving depth perception. In theory, only those structures filled with iodine will have a density greater enough to be visualized. This technique allows for shading of depth and contours. The disadvantage is that this is an all-or-nothing approach. Any voxel above a given threshold will be of equal density to the others, any below that, threshold are eliminated **(Heiken et al., 1997).**

Calcification within a plaque can simulate contrast within the artery and therefore misrepresent stenosis. Furthermore, vessels that are within a contrast enhancing organ, such as vascular tumor, will not be visualized because of overlaying dense contrast enhancement. However, this is the best technique for grading stenosis. Shaded surface displays also tend to be the most useful for evaluation of aneurysms and for displaying of enhanced masses **(Heiken et al., 1997).**

المنارة للاستشارات
www.manaraa.com

Advantage of shaded surface display (SSD):

It provides an excellent view of complex three-dimensional relationships particularly at the regions of overlapping structures (Fig.21) (**Rubin et al., 1995**).

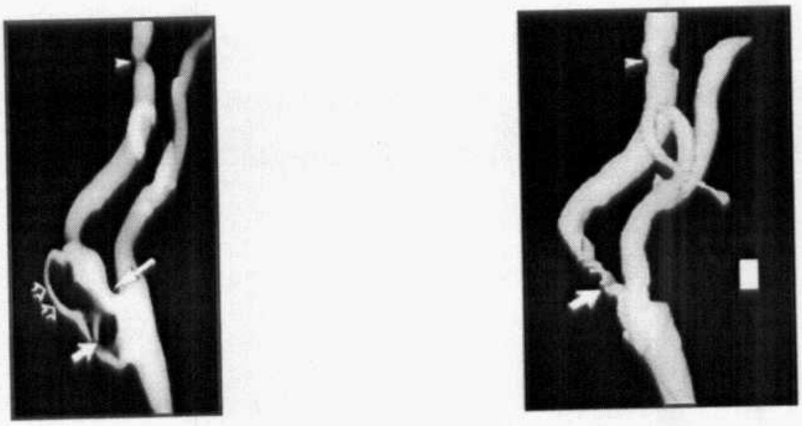

(A) (B)

Figure (21) (A) Spiral VRT CT angiogram of left carotid artery show sever stenosis (long solid arrow). (B) Spiral SSD CT angiogram shows sever stenosis (arrow) (Quoted from Rubin et al., 1995).

Disadvantages of shaded surface display (SSD):

- Threshold selection profoundly affects the vascular appearance. Choosing too low threshold causing noise and makes higher-density soft tissue obscure the target vasculature. On the other hand, choosing too high threshold results in small vessels disappearance and/or stenosis to be falsely implied **(Napel, 1998).**
- Loss of differential attenuation so that structures within the threshold range with different attenuation, fore example

المنارة للاستشارات
www.manaraa.com

calcium in calcified plaque and contrast media cannot be differentiated (**Rubin et al., 1995).**

This could be overcome by manual editing of axial slice but unfortunately, it is subjective and time-consuming **(Thomas et al., 1995).**

B-Maximum intensity projection (MIP):-

It is a technique in which a two-dimensional image is built up. The intensity of each pixel in the resulting image is the maximum intensity encountered along the ray as it traverses the volume (Fig.22) **(Napel, 1998).**

Figure (22) Lateral multiplanar maximum intensity pixel projection CT image clearly depicts the site of the right internal carotid arterial occlusion (arrow). (Quoted from Rubin et al., 1995).

Advantage of maximum intensity projection (MIP):

MIP gray scale reflects relative x-ray attenuation. The absence of thresholding step, as in SSD, ensures that no

www.manaraa.com

information is lost and subtle Variation in attenuation can be appreciated, this has a great importance in the differentiation of calcified atheromas and intra-luminal contrast **(Napel et al., 1992).**

Disadvantage of maximum intensity projection (MIP):

- Single projection image does not encode depth relationships. This shortcoming is countered by the generation of multiple MIPs to enable appreciation of depth relationship (**Rubin et al., 1995**).
- Because MIP always projects the brightest pixel encountered along each ray, bone either in front or behind vascular structure will obscure it. Calcification in the arterial wall, particularly when they are circumferential can present a difficult problem, often obscuring the viewing of the vessel lumen. This is because the use of intravenous injection does not result in higher densities within arteries compared with bone and other calcified structures. So image editing (may be needed in SSD) is used to eliminate bone and other undesirable bright structures **(Napel, 1998).**

This is time consuming and lead to loss of anatomic information **(Thomas et al., 1995).**

المنارة للاستشارات
www.manaraa.com

C-Multi/Curved Planar Reformation:

- Multiplanar reformations are sagittal, coronal and oblique. Curved planar reformation can be very helpful for displaying tortuous vessels that cannot be visualized completely on a flat planar section. Multi and curved planar reformations preserved all of the relative attenuation information (Fig.23).

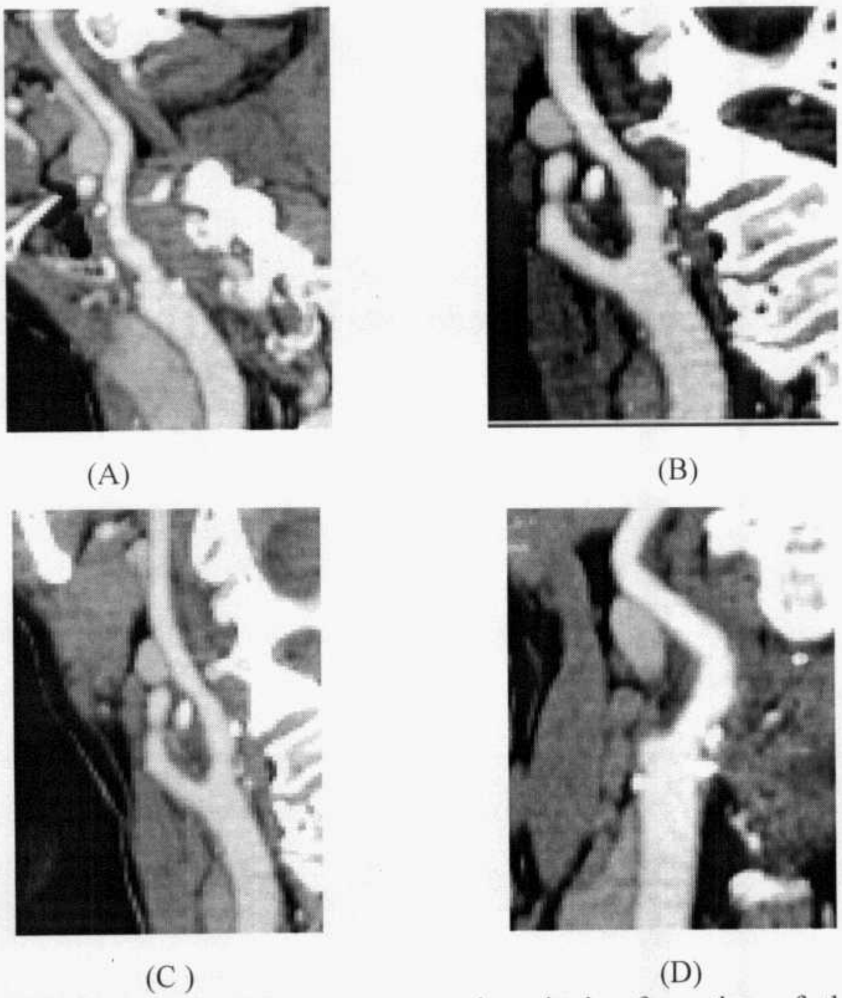

Figure (23): A, B, and C represent normal sagittal reformation of the carotid bifurcation while D represents normal coronal reformation of carotid bifurcation (Quoted from Thomas et al., 1995).

المنارة للاستشارات
www.manaraa.com

They are valuable in visualizing the true walls of blood vessels, their lumen, and the interior of metallic stent. Both techniques are operator dependent, so inclusion or exclusion of voxels due to inaccurate plane section can result in misdiagnosis (**Rubin et al., 1995**).

D-Volume rendering:

Volume rendering is the newest technique to be applied to CT angiography data. It is less popular than MIP and SSD because of its soft and hardware requirements (Ney et al., 1992). Pixel values in the volume of interest are analyzed and the tissues are then given color and transparency depending on the information obtained from the data set. This has the advantages that segmentation is not required prior to rendering and there is no information lost by thresholding (Fig.24) (**Rubin et al., 1995**).

المنارة للاستشارات
www.manaraa.com

(A) (B)

Figure (24) (A) Volume-rendered CT image demonstrates excellent delineation of the artery outlines. (B) Volume-rendered CT image depicts the entire portion of the stenosis (arrowhead) with accuracy despite the calcification. Thereby enables accurate measurement of the stenosis (arrow). (Quoted from Rubin et al., 1995).

Quantitative Vascular Measurements in Arterial Occlusive Disease

For measurement of stenotic occlusion, the residual lumen at the lesion site is compared with the lumen at a reference site. The degree of occlusion is measured in terms of the diameter or area of stenosis. The percentage of stenosis is calculated as $(1 - L/R) \times 100$, where L and R are the area or diameter of the lesion and of the reference site, respectively **(Hideki Ota et al., 2005).**

المنارة للاستشارات
www.manaraa.com

Reference Site

There are two methods of assigning the reference site (Fig.25). In the first method, a normal-looking portion of the stenotic vessel either proximal or distal to the lesion serves as the reference site. In the second method, the reference site is located at the level of the lesion. The percentage of stenosis may differ according to the location of the reference site **(Naylor AR et al., 2003).**

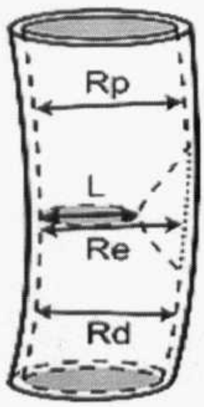

Figure (25) Drawing illustrates measurements used to determine the degree of vascular stenosis. *Rp* and *Rd* indicate the luminal diameter or area in the normal-looking portion of the vessel proximal *(Rp)* and distal *(Rd)* to the stenotic lesion *(L)*. *Re* is the estimated luminal diameter or area at the level of the lesion. Any of these values—*Rp*, *Rd*, or *Re*—can be used as the reference value, and it should be noted which of the three is used. (Quoted from Hideki Ota et al., 2005).

المنارة للاستشارات
www.manaraa.com

Diameter Stenosis

Traditionally, only diametric measurements have been used for the evaluation of stenosis because the images provided by catheter-based angiography, which for many years has been the standard of reference in this setting, are projection images of the affected vessel, making diameter stenosis measurable but not area stenosis. For evaluating diameter stenosis, the minimum luminal diameter at a target site is determined. The projection image should be generated at an angle that allows measurement of the minimum luminal diameter; this dimension may be unmeasurable in cases of eccentric stenosis with images generated at suboptimal angles (Fig.26). In contrast, on cross-sectional images, the minimum luminal diameter can be measured accurately without difficulty (Fig.24) **(Hideki Ota et al., 2005).** .

المنارة للاستشارات
www.manaraa.com

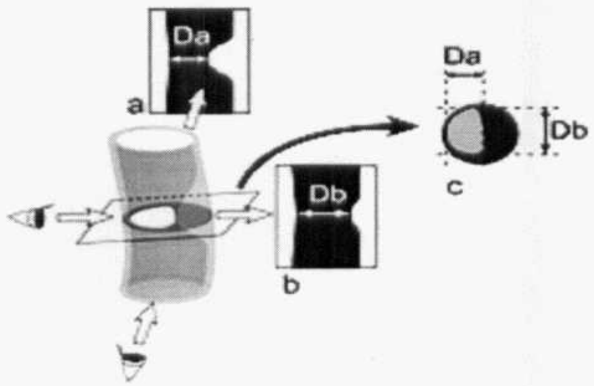

Figure (26). Drawings illustrate how projection images *(a, b)* and a cross-sectional image *(c)* are used to measure the diameter of an eccentric arterial stenosis. In *a*, the minimum luminal diameter *(Da)* is depicted at the optimal projection angle. In *b*, the degree of stenosis is underestimated because the minimum luminal diameter *(Db)* is depicted at a suboptimal projection angle, making it larger than *Da*. The cross-sectional image is oriented perpendicular to the vessel and accurately depicts lumen morphology, making the minimum luminal diameter easy to measure. *Da* and *Db* in *c* correspond to the diameters measured (Quoted from Hideki Ota et al., 2005).

Area Stenosis

Some reports state that a reduction in cross-sectional area correlates better with the hemodynamic effect of stenosis than does a reduction in diameter. Therefore, change in cross-sectional area has been proposed as a more accurate way of measuring arterial stenosis. Evaluation with true cross-sectional images that are oriented perpendicular to the affected vessel is essential for quantification of area stenosis. Such evaluation is relatively time consuming if the border of the lumen is traced manually. Software programs (eg, Advanced Vessel Analysis; GE Medical Systems) are now commercially available that can

www.manaraa.com

measure area stenosis automatically and help reduce the amount of time required for analysis **(Hideki Ota et al., 2005).**

Relationship between Diameter and Area Stenosis

It is important to note whether an arterial stenosis is measured in terms of diameter or area because the two percentages do not correspond (Fig.27) illustrates the relationship between area reduction and diameter reduction in cases of completely concentric stenosis: The degree of area reduction is greater than the degree of diameter reduction, unless there is either no stenosis (0% reduction) or total occlusion (100% reduction). In cases of eccentric stenosis, the relationship between area and diameter reduction is not constant **(Naylor AR et al., 2003).**

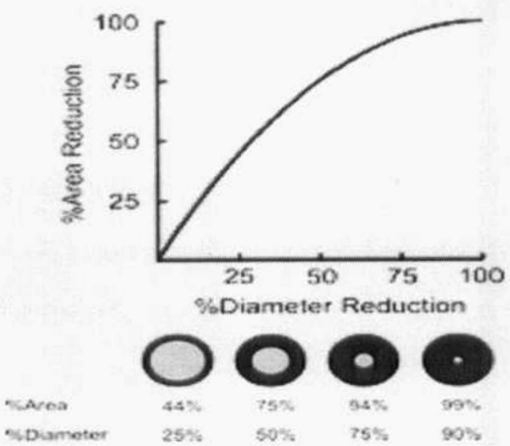

Figure (27). Graph (top) illustrates the relationship between area reduction and diameter reduction in a completely concentric stenosis. (Quoted from Hideki Ota et al., 2005).

www.manaraa.com

Patients, Materials and Methods

The study was performed at radiology department of Al-Hossein University Hospital over the period from November 2004 to August 2005.

- Patients suffering from symptoms and signs suggestive of thromboembolic stroke, were referred from stroke unite of neurology department, Al-Hossein University Hospital, patients with a history of transient ischemic attacks (TIAs) and non-symptomatic patients of high risk developing atherosclerosis. In addition, patients with symptoms suggestive of extra-cranial carotid artery affection,(such as pulsating swelling in the neck).

- Patients were subjected to scanning using CT scanner Hispeed QX/I (4 slices), General Electric Health care Technology, U.S.A

رات
:om

All patients were subjected to:

A) Clinical evaluation, including:

I. Full history tacking:

a. Personal history: name, age, sex, and smoking.

b. Complain, onset, course, and duration.

c. History of present illness.

d. Past history of similar attacks and associated disease.

II. General examination: with special attention for pulse, blood pressure and conscious level.

III. Local examination of the neck for presence or absence of carotid pulsation, equality of pulsation, palpable thrill, and neck swellings, which might distort the anatomy.

B) Non-radiological investigations:

1. Fasting and postprandial blood sugar.
2. Serum cholesterol and triglycerides.
3. Serum creatinine.

رات
:om

C) **Radiological and imaging investigations:**

1. Bilateral carotid color coded duplex.
2. Non-contrast axial CT scan of the brain.
3. ***CT angiography***

Carotid artery CT angiography protocol	
Specific Anatomic Region	Extracranial carotid arteries
Contrast volume and type	100-120ml of non-ionic contrast medium
Flow rate	4ml/sec.
Area scanned	Base of skull till C5-6
Scan Delay	Determined by preliminary bolus injection of 2oml contrast media or by using smart prep*. technique
Total scan time	30 seconds
Slice thickness	1.25mm
Reconstruction interval	1.25mm

رات
:om

Table speed/pitch	3.75 mm /rot. with a pitch of 0.75
Scanner used	G.E. High speed (4detectors)
Field of view	22cm
Other parameters	map=220, kvp=120

Patients were asked to avoid swallowing, but quiet breathing was allowed throughout the examination.

****Smart prep technique*** (software; GE Medical Systems):

An automatic triggering system was used to detect a bolus of contrast material in selected region of interest (ROI), and start scanning at maximum contrast enhancement of the vessels though the following steps.

1. Scout view.
2. Single axial cut at the level of aortic arch.
3. Select the region of interest (ROI) at the aortic arch in the axial cut.
4. Start monitoring phase and contrast injection at the same time.

5. Start scanning phase when contrast density at the region of interest (ROI) >50 HU (Fig.28).

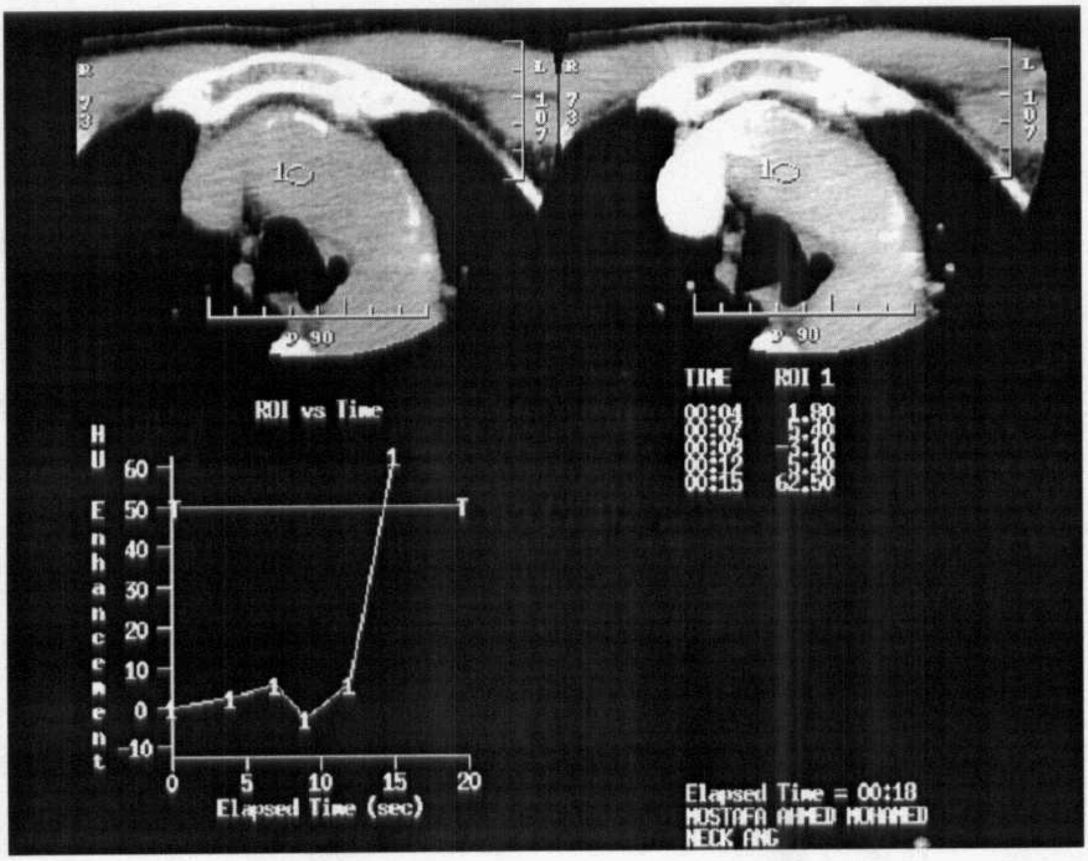

Figure (28) Smart prep technique, show (ROI) at aortic arch and scanning started when contrast density >50 HU at (ROI).

CT angiography pos-processing. With Shaded Surface Display(SSD), Maximum intensity projection (MIP), Multi/Curved Planar Reformation and Volume rendering (VR) techniques. These techniques were discussed in details in chapter CT angiography technique.

www.manaraa.com

<u>The percentage of stenosis is calculated by using Advanced vessels analysis technique</u>. *(*Software; GE Medical Systems*)*.

The most stenotic area and distal nonstenotic area were analyzed by acquiring multiplanar reconstruction (MPR) images at 3D CT angiography through the following steps by using curved reformat (Fig.29).

- Select the reference point at distal non stenotic area.
- Select the start of stenosis point.
- Select the end of stenosis point .
- Then the most stenotic area and distal reference nonstenotic area will be automatically analyzed to obtain the percentage of stenosis depending on area diameter.

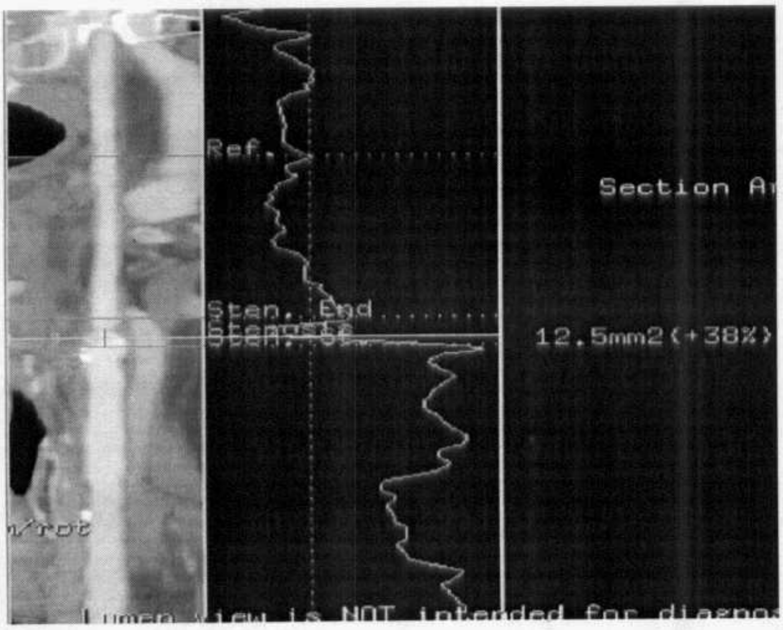

www.manaraa.com

Figure (29): Advanced vessels analysis technique .

The CTA findings of each ICA is graded according to North American Symptomatic carotid Endarterectomy Trial criteria to:

I- normal;

II - (1%–29%), mild stenosis.

III- (30%–69%) , moderate stenosis.

IV- (70%–99%), severe stenosis.

V- Complete occlusion.

The length of stenosis was measured on multiplanar reconstruction images. The appearance of the plaque surface was assessed on reconstructed images by studying the interface between the plaque and the vascular lumen.

رات
:om

Results

This study was performed on 28 patients representing 56 carotid systems with age ranging from 35 to 70 years. 11 were females and 17 were males.

Table (1): Represents the age and sex distribution.

Age group	Sex				Total	
	Male		Female			
	No	%	No	%	No	%
<39	1	6.3	1	3.6	2	7.2
40-49	3	10.7	2	7.2	5	17.9
50-59	3	10.7	6	21.4	9	32.1
60-69	19	32.0	2	7.2	11	39.2
70-79	1	3.6	-	-	1	3.6
>79	-	-	-	-	-	-
Total	17	60.8	11	39.2	28	100

According to their clinical presentation in relation to sex they are classified as shown in table (2).

Table (2):

Presentation	Male		Female		Total	
	No	%	No	%	No	%
C.V.S.	10	35.7	6	21.4	16	57.1
T.I.As	6	21.4	4	14.3	10	35.7
Pulsating swelling	1	3.6	-	-	1	3.6
Asymptomatic	-	-	1	3.6	1	3.6
	17	60.7	11	39.3	28	100

C.V.S. = Cerebro Vascular Stroke.

T.I.As. = Transient ischaemic attacks.

راث
:om

According to C.T. finding they are classified as shown in table (3).

Table (3):

C.T. finding	sex				Total	
	Male		Female			
	No	%	No	%	No	%
Normal	10	35.8	3	10.7	13	46.5
Recent infarction	6	21.4	4	14.25	10	35.7
Lacunar infarcts	1	3.6	4	14.25	5	17.8
	17	60.8	11	39.2	28	100

رات
:om

Carotids (56) are classified according to CTA finding as shown in table (4).

Table (4):

Group	Lesion	No	%
Group I	Normal	21	37.4
Group II	Stenotic lesions	31	55.3
Group III	Total occlusion	3	5.4
Group IV	Non stenotic lesions	1	1.8
Total		56	100

ارات
:om

According to pervious table (Table 4) Stenotic lesions were further classified according to the percentage of stenosis as follows.

Table (5):

Percentage of stenosis	No. of carotids	%
Mild stenosis (1-29%)	14	45.2
Moderate stenosis (30-69%)	12	38.7
Sever stenosis (70-99%)	5	16.1
Total	31	100

رات
:om

ICAs (56) were classified according to conventional and color flow duplex sonography finding as shown in table (6).

Table (6):

group	Lesion	No	%
Group I	Non stenotic ICAs <40%	38	67.8
Group II	Stenotic ICAs 40-99%	14	25
Group III	Total carotid occlusion%	3	5.4
Group IV	Non stenotic lesions	1	1.8
Total		56	100

N.B.:
-Non stenotic carotids include normal carotids and those with plaques of less than 40% stenosis.
-Non stenotic lesions include lesions other than stenosis, like Arterio-venous fistula

:om

According to pervious table (Table 6) Stenotic lesions were further classified according to the percentage of stenosis as follows.

Table (7):

Percentage of stenosis	No. of carotids	%
Moderate stenosis (40-69%)	9	64.3
Sever stenosis (70-99%)	5	35.7
Total	14	100

:om

Case No. 1

Male patient 55 years old, presented by right sided hemiparesis.

Not diabetic or hypertensive.

C.T brain: Right basal ganglia infarct.

Conventional and color flow duplex sonography:

The main abnormality is increase IMT.

CT angiography :

CT angiography was done with axial images reconstruction, using nontransparent (Fig.30A) and transparent (Fig.30B) volume render techniques, parasaggital reformat by means of maximum intensity projection (MIP) (Fig.30C), and shaded surface display (SSD) (Fig.30D).

These techniques show normal caliber of both common and internal carotid arteries with no evidence of stenosis or atheromatous formation.

رات
:om

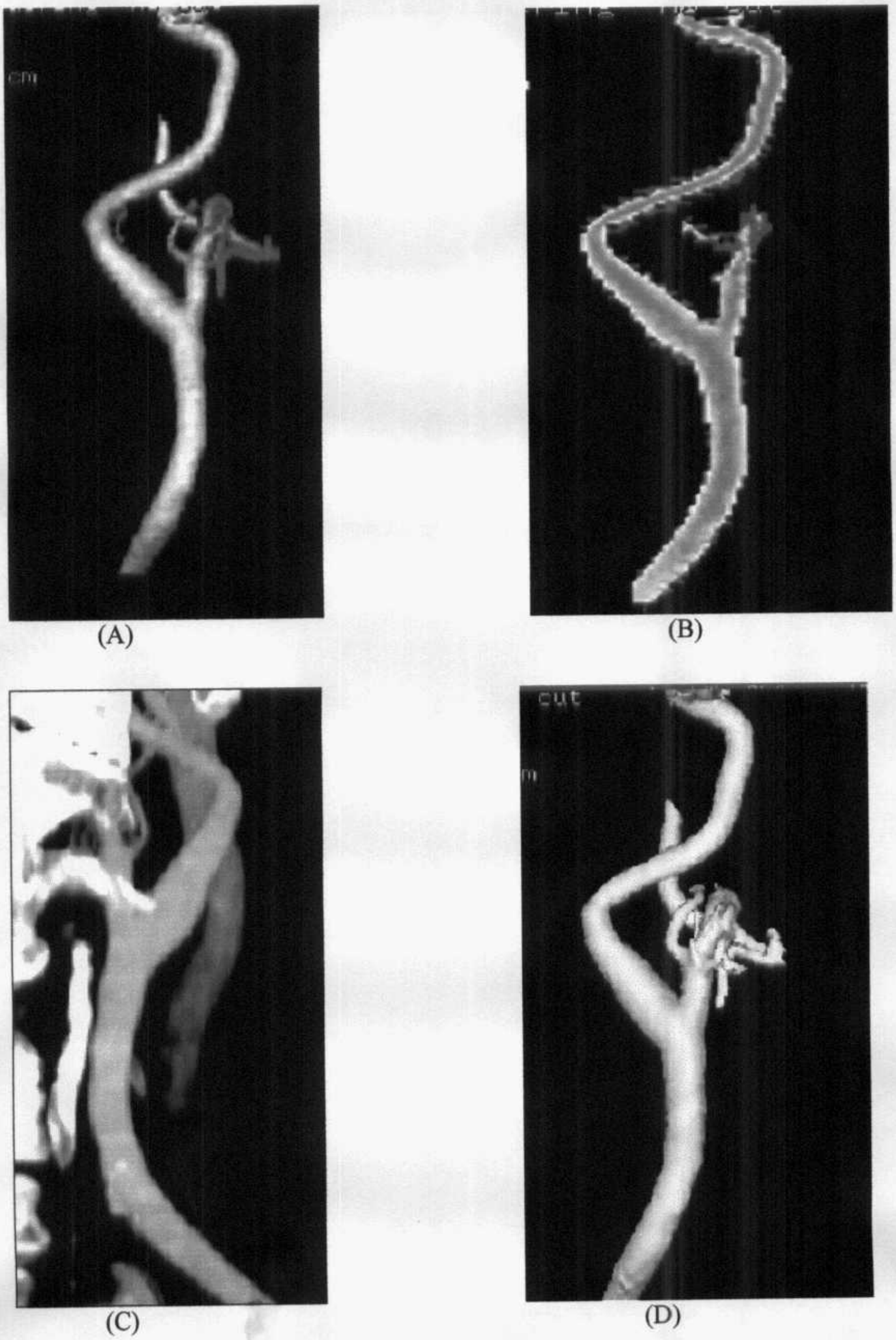

Figure (30): Normal caliber of left CCA and ICA by nontransparent (A) and transparent (B) VRTs, maximum intensity projection reformate (MIP) (C), and shaded surface display (SSD) (D)

المنارة للاستشارات
www.manaraa.com

Case No. 2

Male patient 72 years old presented by TIAs.

Not diabetic or hypertensive.

Elevated cholesterol and triglycerides.

CT brain.: Age related evolutional changes.

Conventional and color flow duplex U/s:

Large fibro fatty atheromatous plaque with lumen reduction 70 % is noted at right ICA (Fig.31E).

CT angiography

CT angiography with parasaggital reformat by means of maximum intensity projection (MIP) (Fig.31A), shaded surface display (SSD) (Fig.31B), volume render technique (VRT) (Fig.31C), and curved reformat (Fig.31D). These techniques show 69% stenosis with ulcer (White arrow) at the origin of right internal carotid artery, 2.1cm in extent.

In addition, there is mild external carotid artery stenosis (yellow arrow).

المنارة للاستشارات
www.manaraa.com

(A) (B) (C)

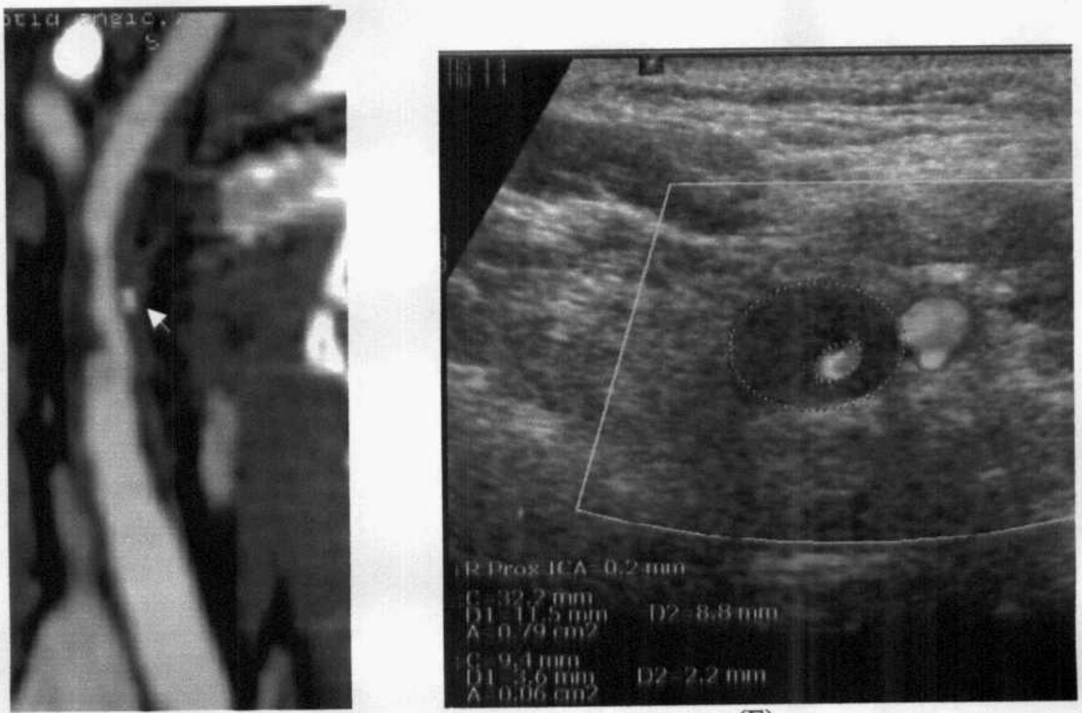

(D) (E)

Figure (31): Right internal carotid stenosis with ulcer (Wight arrow) by MIP parasaggital reformat (A), SSD (B), VRT (C), curved reformat (D), and color Doppler U/S (E). Right external carotid artery stenosis is additionally noted (yellow arrow).

المنارة للاستشارات
www.manaraa.com

Case No. 3:

Male patient 73 years old presented by right sided hemiparesis.

Diabetic and hypertensive.

Elevated levels of triglycerides and cholesterol.

CT brain; left temproparietal infarction (extensive) at the distribution of middle cerebral artery.

Conventional and color flow duplex U/S:

There is absent color flow at distal left ICA. (Fig.32D)

CT angiography:

Parasaggital helical CT angiography images reformated by means of a volume rendering (Fig.32A) and maximum intensity projection (Fig.32B) techniques followed by spiral VRT (Fig.32C) were done. It reveals:

Complete Left internal carotid artery occlusion. The site of the occlusion is well demonstrated (arrow)

المنارة للاستشارات
www.manaraa.com

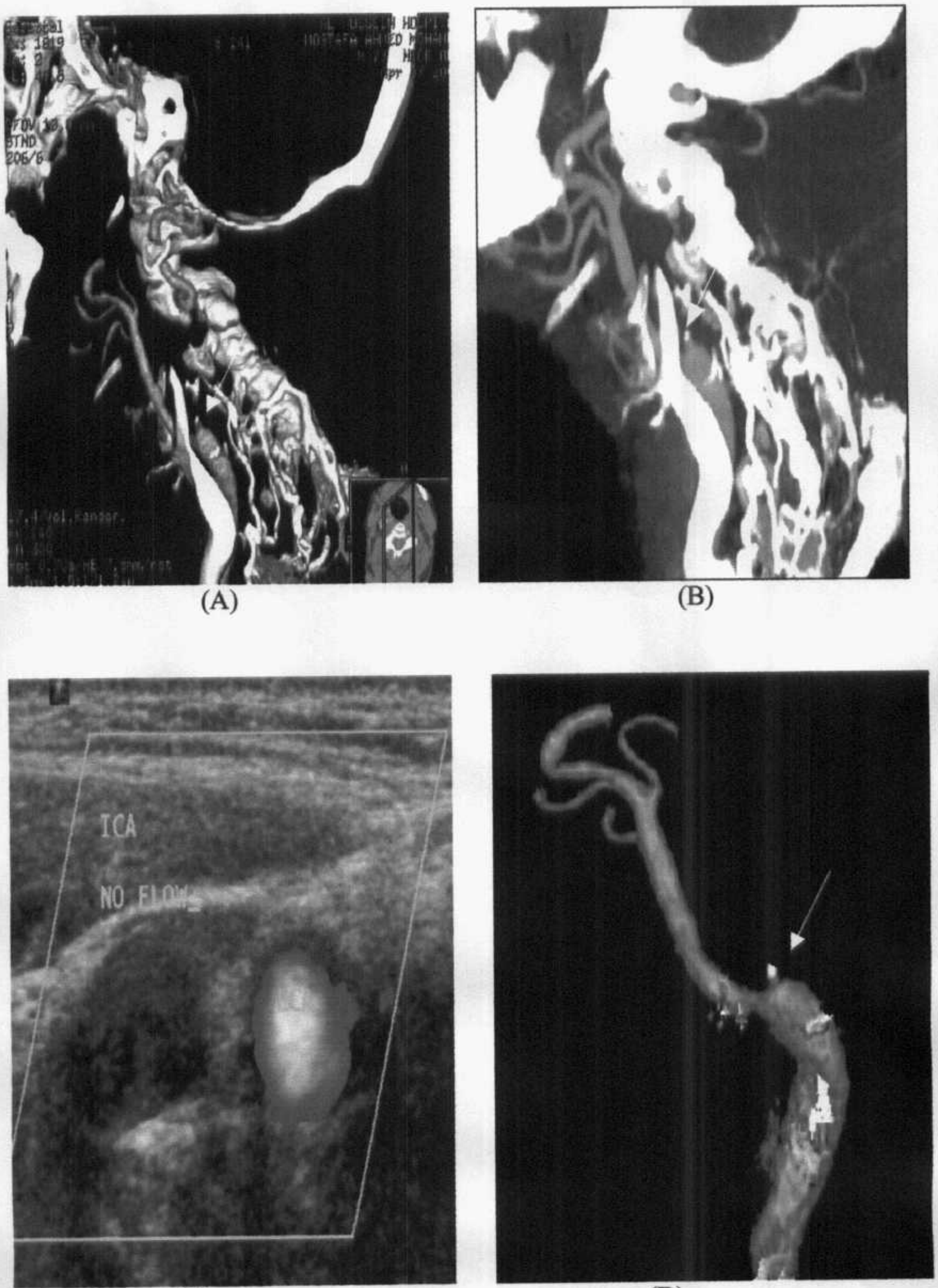

(A) (B) (C) (D)

Figure (32): Complete occlusion of ICA by Parasaggital images reformed by means of a volume rendering (A) and maximum intense projection (B), spiral VRT (C) and color flow Doppler (D)

المنارة للاستشارات
www.manaraa.com

Case No.4:

Male patient 67 years old presented by TIAs.

Not diabetic or hypertensive

Normal blood sugar, elevated cholesterol and triglycerides levels.

CT brain : Left lacunar infarcts.

Conventional and color flow duplex U/S:

There is fibrous plaque at the wall of left internal carotid artery (fig.33E).

CT angiography:

CT angiography using volume render technique (VRT) (Fig.33A), shaded surface display (SSD) (Fig.33B), and Curved planner reformat (Fig.33C), these techniques show stenosis at the origin of internal carotid artery 2.5cm in extent (arrow). The percentage of stenosis is 49%.

Axial CT reformat image obtained at the level of the Stenosis (Fig.33D) shows the max and min diameters of stenosed segment.

Digital subtraction angiography (DSA) was done (Fig.33D) and representing a good correlation with CT angiographic findings.

المنارة للاستشارات

www.manaraa.com

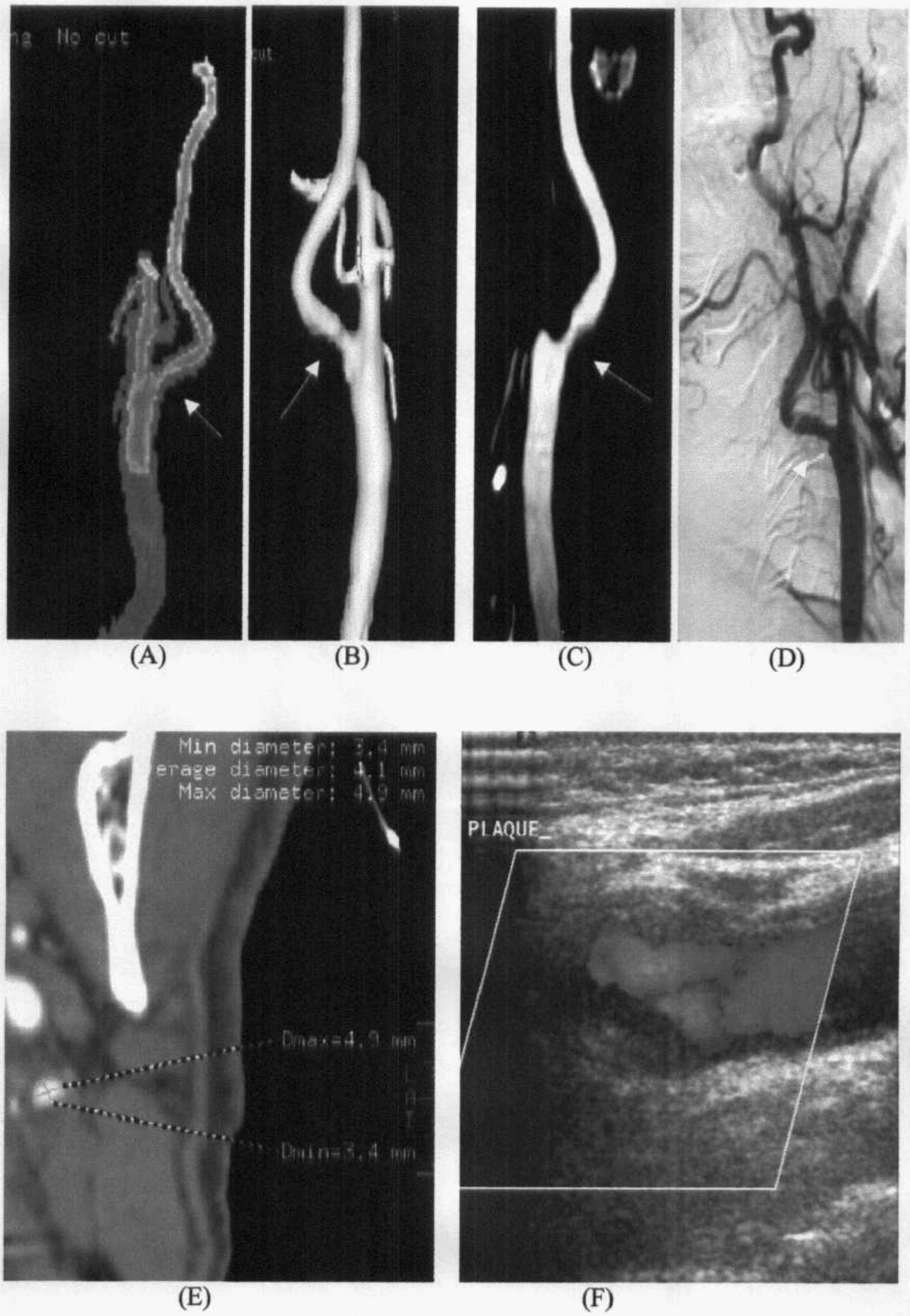

Figure (33): Left ICA stenosis by volume render technique (A), shaded surface display (B), Curved planner reformat (C)Digital subtraction angiography (D), axial CT reformat (E) and color flow Doppler (F).

www.manaraa.com

Case No.5

Female patient 56 years old presented by TIAs.

Diabetic

Elevated level of serum cholesterol and triglycerides

CT brain: Normal.

Pulsed wave Doppler U/S:

	PSV	EDV
ICA	111.8	18.1

These velocities indicate stenosis of 40-59 %. (Fig.34D)

CT angiography:

CT angiography using transparent (Fig.34A) and non transparent (Fig.34B) volume render techniques, and curved reformat (Fig.34C) were done. These techniques show calcified plaques with 42% stenosis at the origin of left internal carotid artery, 1.8cm in extent (arrow).

المنارة للاستشارات
www.manaraa.com

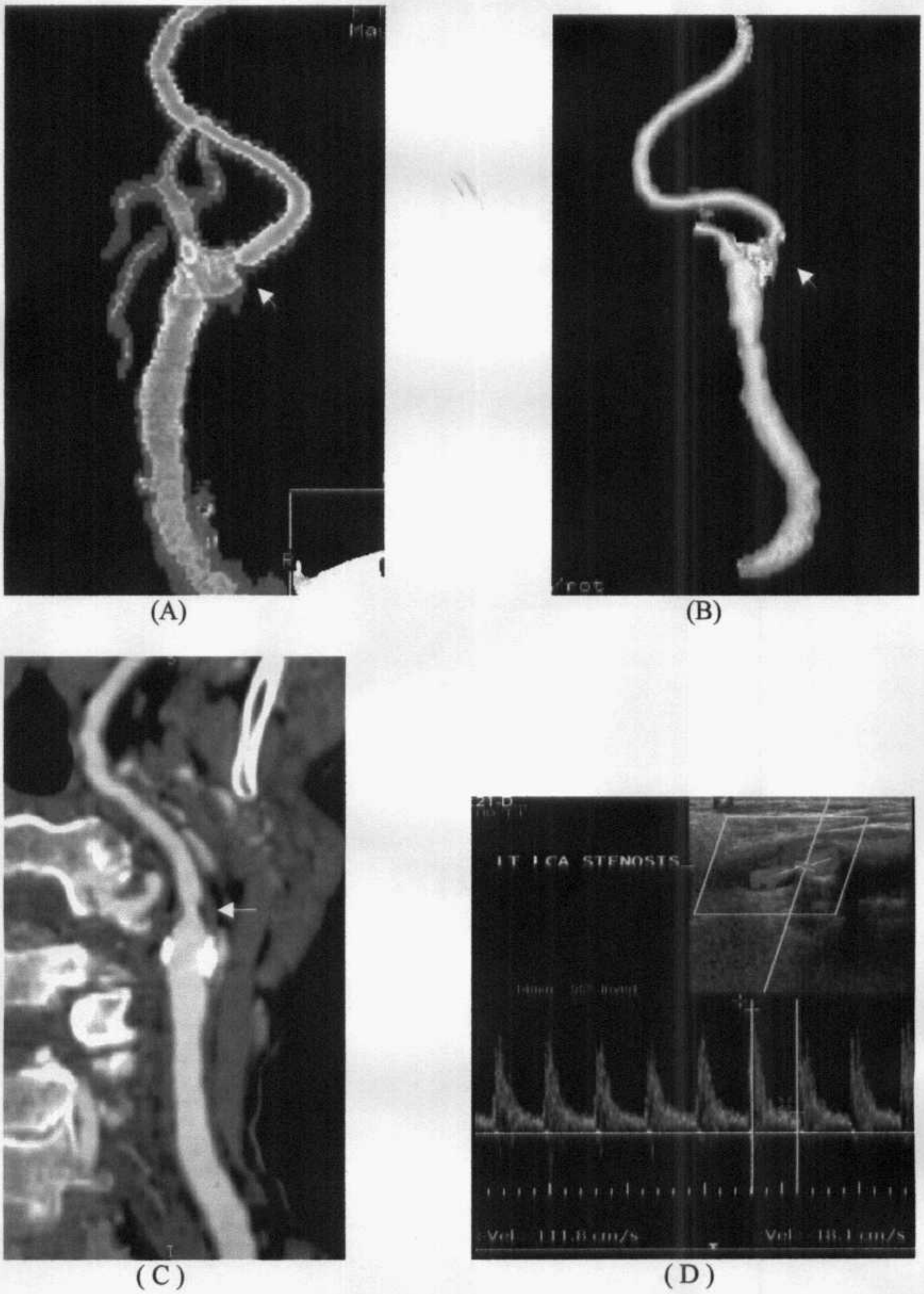

Figure (34): Left internal carotid artery stenosis by transparent (A) and non transparent (B) volume render techniques, curved reformat(C), and pulsed wave Doppler of ICA (D).

www.manaraa.com

Case No.6:

Male patient 35 years old presented with pulsating swelling in the right side of the neck.

Past history of stab wound to the right side of the neck 6 month ago.

CT brain: Normal

Conventional and color flow duplex U/S:

Right common carotid arterial pseudoaneurysm with fistula to the right internal jugular vein and turbulence of blood flow (Fig.35D)

Ct angiography :

CT angiography was done. Transverse axial images were reconstructed by means of coronal maximum intense projection (MIP) (Fig.35A), volume render techniques (VRT) (Fig.35B), and shaded surface display (SSD) (Fig.35C) depict an extravascular collection of contrast agent arising from the right common carotid artery, which represents a pseudoaneurysm with fistula to internal jugular vein . The right IJV appears prematurely opacified.

المنارة للاستشارات
www.manaraa.com

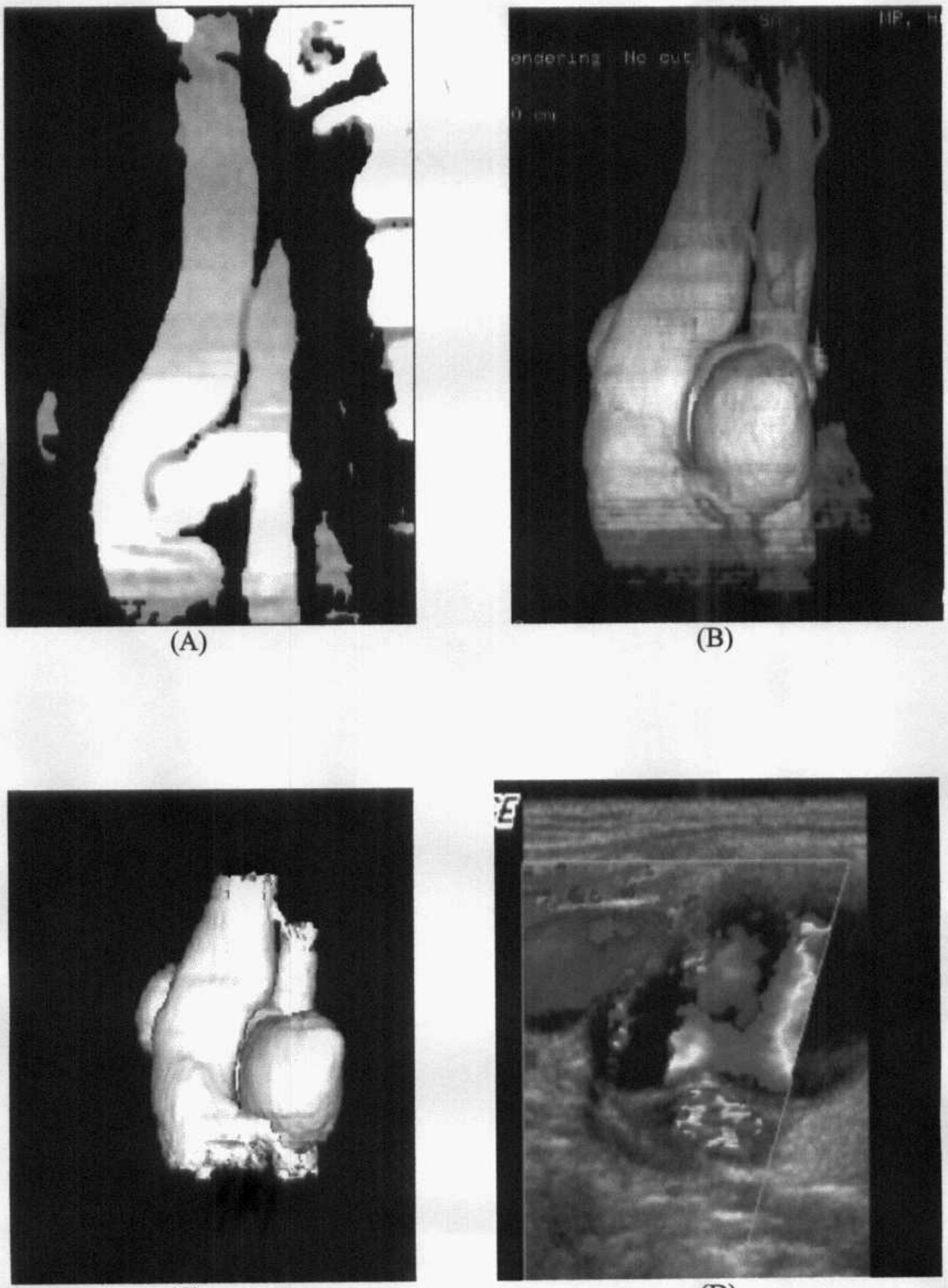

(A) (B)

(C) (D)

Figure (35):Right common carotid arterial pseudoaneurysm with fistula to the right internal jugular vein by coronal reformat (MIP) (A), volume render(B), shaded surface display (SSD) (C), and color flow duplex (D)

المنارة للاستشارات
www.manaraa.com

Case No 7:

Male patient 62 years old presented by right sided hemiparesis.

Hypertensive.

Elevated serum cholesterol and triglycerides

CT brain : Age related atrophic changes, no acute infarct.

Conventional and color flow duplex U/S:

Small fibrous plaques at the proximal part of left ICA (Fig.36E).

CT angiography:

CT angiography with transparent (Fig.36A) and non transparent (Fig.36B) volume render techniques, and curved reformat (Fig.36C) were done. These techniques show proximal left internal carotid artery stenosis 1.2cm in extent (20% stenosis) (arrow),

Digital subtraction angiography (DSA):

(DSA) was done (Fig.36D) and good correlation between the angiogram and CT angiography was found.

www.manaraa.com

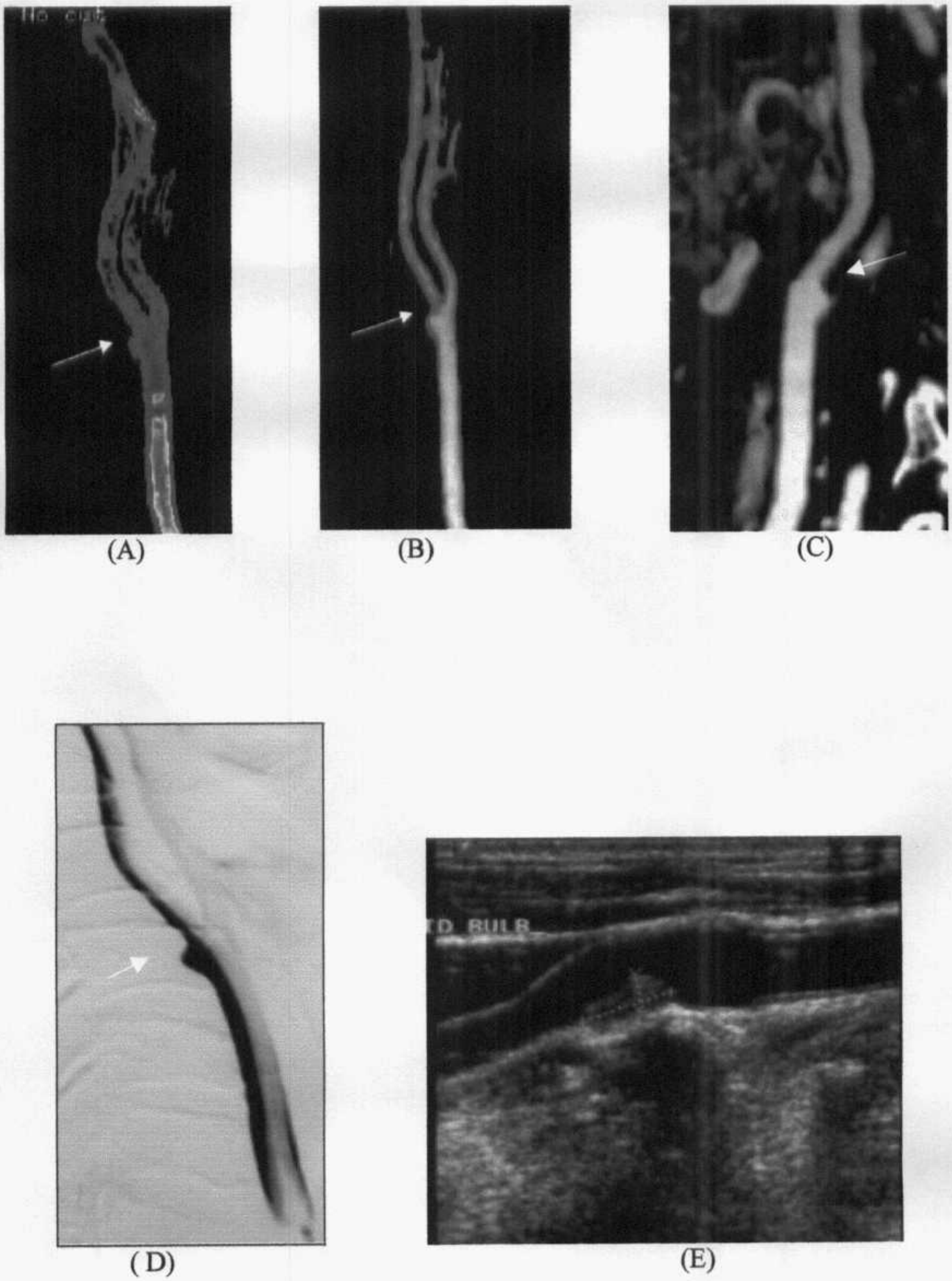

Figure (36): Left internal carotid artery stenosis by transparent (A) and nontransparent VRTs (B), Curved reformat(C) Digital subtraction angiography (DSA) (D), and B-mode ultrasound(E).

المنارة للاستشارات
www.manaraa.com

Case No.8:

Male patient 67 years old presented by left hemiplegia

Diabetic with fasting blood sugar 160mg/dl.

CT brain: right parietal infarction

Conventional and color flow duplex U/S:

Calcified fibrous plaque at the proximal part of right internal carotid artery with lumen reduction (Fig.37E).

CT angiography:

CT angiography was done with axial images reconstruction and 3D CTA using maximum intensity projection (MIP) technique (Fig.37B). In MIP technique, stenosis could not be assessed because of calcification.

The axial CT reformat (Fig.37D) clearly differentiates concentric calcification from vascular lumen. In addition, curved reformat (Fig.37C) shows sever stenosis at the origin of right internal carotid artery. The percentage of stenosis is 65%

Digital subtraction angiography was done (Fig.37A) and representing a good correlation with CT angiographic findings.

المنارة للاستشارات
www.manaraa.com

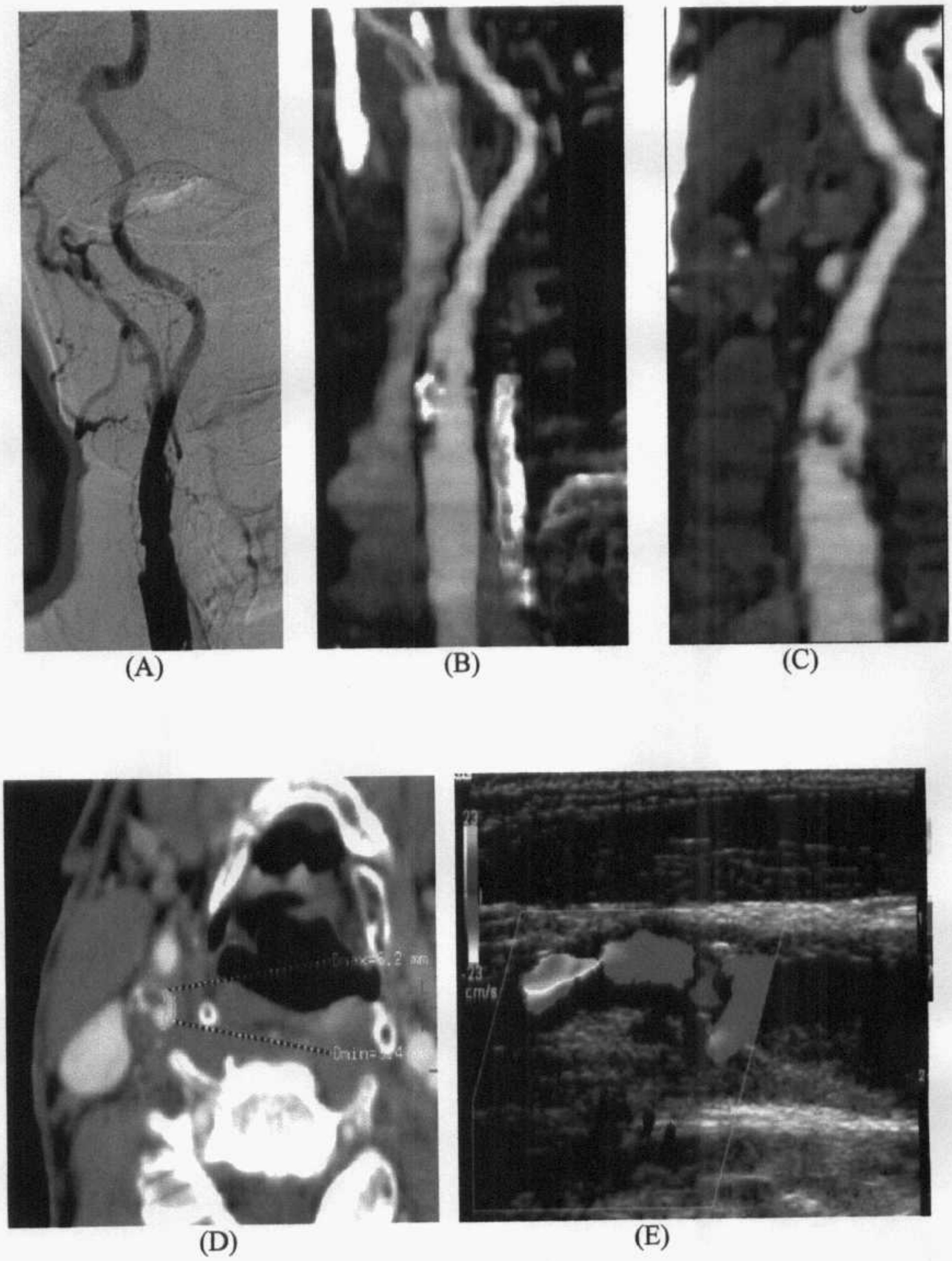

Figure (37): Right internal carotid artery stenosis by DSA (A), MIP(B), curved reformat(C), axial CT reformat (D), and color flow duplex (E)

المنارة للاستشارات
www.manaraa.com

Case No.9:

Female patient 59 years old presented by TIAs.

Not diabetic or hypertensive.

Elevated serum cholesterol and triglycerides.

CT brain: Age related evolutional changes.

Pulsed wave Doppler of ICA (Fig.38E) shows the following

	P.S.V	E.D.V
Right ICA	132.6	22.5

These velocities indicate stenosis of 40-59%.

CT angiography:

CT angiography with non transparent (Fig.38A) and transparent (Fig.38B) volume render techniques, and curved reformat (Fig.38C). These techniques show calcification and 52% stenosis at the origin of right internal carotid artery1.1cm in extent (arrow).

In addition, axial reformat (Fig 38D) at the level of stenosis, demonstrate its max. and min. axial diameters

www.manaraa.com

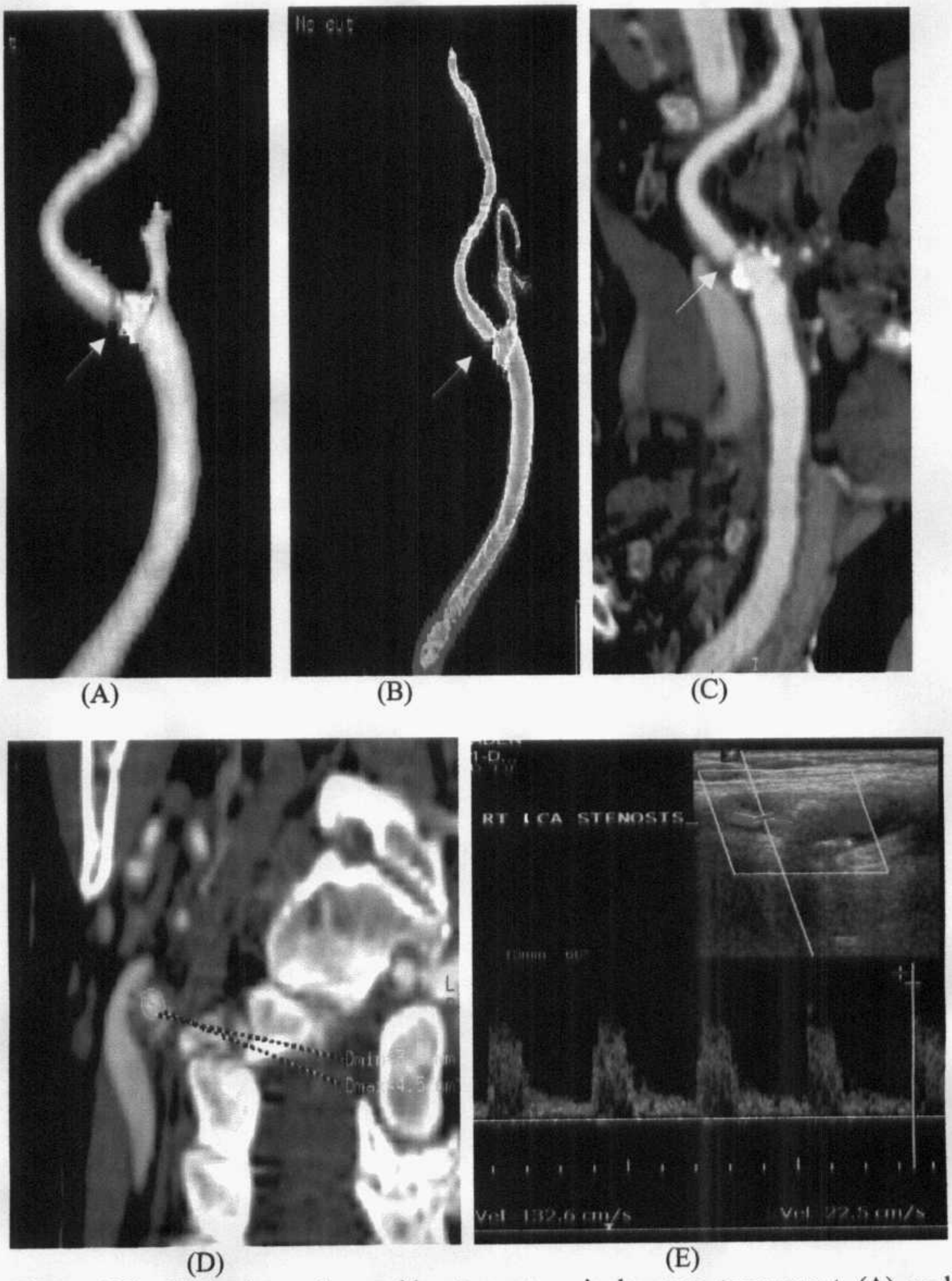

Figure (38): Right internal carotid artery stenosis by non transparent (A) and transparent (B) volume render techniques , curved reformat (C), axial reformat (D), and pulsed wave Doppler U/S (E).

www.manaraa.com

Case No 10:

Female patient 61 years old presented by TIAs.

Diabetic with fasting blood sugar 150 mg/dl

Normal cholesterol and triglycerides.

CT brain : Normal.

Conventional and color flow duplex U/s: reveals.

Fibro fatty atheromatous plaque with lumen reduction (28% stenosis) at left ICA. (Fig.39D).

CT angiography

CT angiography was done. Transverse axial images were reconstructed by means of volume render technique (VRT)(Fig.39A), shaded surface display (SSD)(Fig.39B), and maximum intensity projection of parasaggital reformat (MIP)(Fig.39C).

These techniques show 30% stenosis at the proximal part of left internal carotid artery, 3cm in extent (arrow)

المنارة للاستشارات
www.manaraa.com

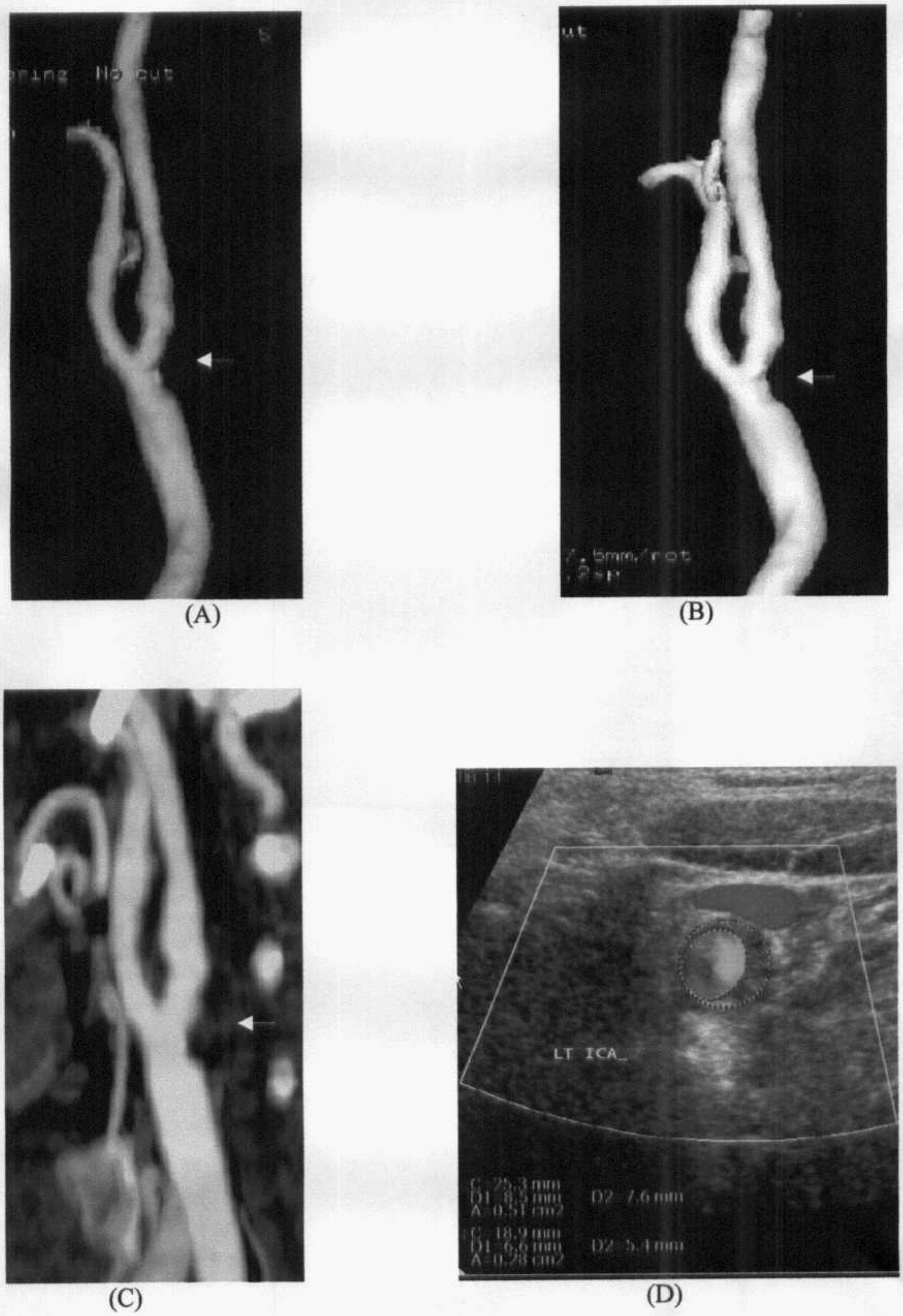

Figure (39) Left internal carotid artery stenosis by VRI (A), SSD (B), MIP parasaggital reformat (C), and color flow duplex U/S (D)

www.manaraa.com

Case No 11.

Male patient 73 years old presented by left sided hemiparesis

Diabetic and hypertensive.

Fasting blood sugar 170mg/dl

Cholesterol 275mg/dl

CT brain: Right tempropariental infarction (extensive) at the distribution of middle cerebral artery.

Conventional and color flow duplex U/s:

B-mode: Sonolucent right ICA lumen (Fig.40E).

CT angiography:

CT angiography with parasaggital reformats by means of maximum intensity projection (MIP) (Fig.40A) and volume render techniques (Fig.40B) and selective spiral volume render technique (Fig.40 C).

These techniques show complete right internal carotid artery obstruction (arrow).

Digital subtraction angiography (DSA):

(DSA) was done (Fig.40D) and good correlation between the angiogram and CT angiography was found.

www.manaraa.com

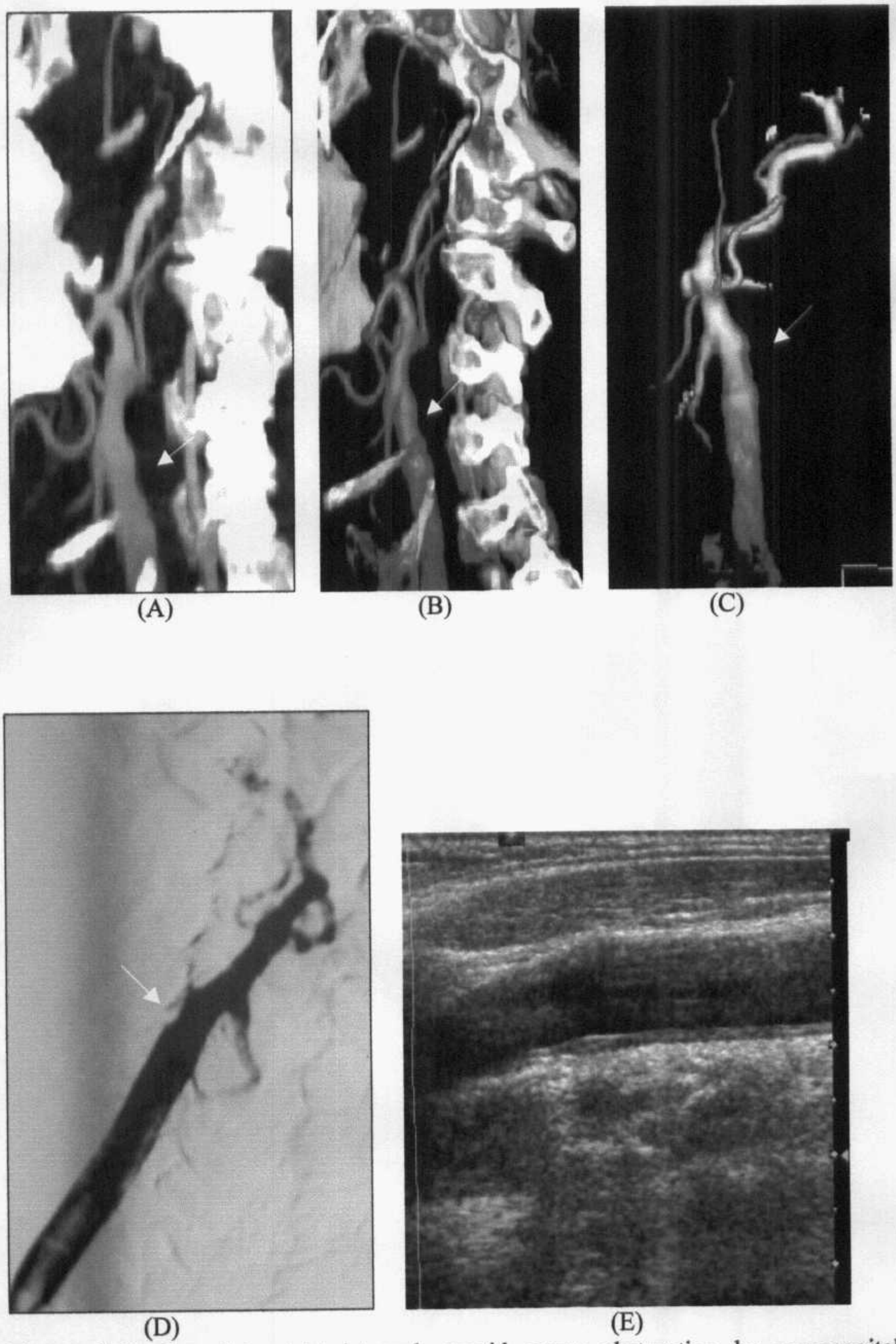

Figure (40): Complete right internal carotid artery obstruction by parasaggital reformats by MIP (A) and VRT (B), selective volume render technique (C), DSA (D) and B-mode U/S (E).

www.manaraa.com

Discussion

The risk of stroke could be reduced by performing carotid endarterectomy in symptomatic patients with a stenosis of more than 70%. Furthermore, endarterectomy in patients with asymptomatic moderate carotid stenosis of 50%–69% produced moderate reduction in the risk of stroke. Asymptomatic Carotid Atherosclerosis Study suggested that asymptomatic patients could benefit from carotid endarterectomy, even with a stenosis of 60% **(Barnett HJ.et al.,1998).**

Other factors are also important in determining whether a carotid lesion will remain clinically silent. Plaques that are more prone to disruption, fracture, or fissuring may be associated with a higher risk of embolization, occlusion, and consequent ischemic neurologic event (**Hatsukami TS. et al., 1997**).

Digital subtraction angiography (DSA) is the gold standard for the evaluation of carotid artery disease. However, because of the risks and the costs of this procedure, noninvasive techniques, such as computed tomographic (CT) angiography has been developed (**Bruno Randoux et al., 2001**).

DSA has well-known risks and limitations. DSA allows only a limited number of views, which can lead to an underestimation of the degree of stenosis **(Ho VB et al., 1998).**

DSA is also a relatively expensive technique, there is a small but definite risk for major complications secondary to the procedure itself. The Asymptomatic carotid Atherosclerosis Study Committee reported a 1.2% risk of persisting neurologic deficit or death following DSA, while the surgical risk was 1.5%. The North American Symptomatic Carotid Endarterectomy Trial showed an overall perioperative risk of persisting neurologic deficit or death of 5.8% (selective angiography accounting for 0.7%). For these reasons, there is a need for accurate noninvasive techniques as alternatives to DSA in evaluation of carotid stenosis **(Ho VB et al., 1998).**

Helical computed angiography (CTA) is a safe, noninvasive technique that allows the rapid acquisition of data that can be reconstructed into two- and three- dimensional images. CTA examination take only a few minutes, non invasive, requires only IV contrast injection, the reconstructed images can shown in film reading sessions, and the anatomy which has a similar appearance to that shown by angiography, is easy to understand **(Link et al., 1997).**

Helical CT with 3D reconstruction produces angiographic like images and is accurate in evaluating the degree of ICA stenosis despite the radiation dose and need for iodinated contrast material administration. This technique is based on a rapid acquisition of the entire volume owing to the continuous

رات
:om

rotation of the gantry and simultaneous displacement of the examination table. Data acquisition by using narrow collimation can be reconstructed with overlapping sections; this provides high spatial resolution **(Xavier Leclerc et al., 1999).**

Good image quality is essential. All CT angiographic images obtained in our study were of diagnostic quality. A CT angiographic image of good quality is easily obtained if the patient does not move or swallow for 1 minute. In addition, by using automatic triggering with detection of the contrast material bolus, we were able to selectively obtain an arterial phase image.

Our study was carried out on 28 patients (56 carotid systems). They are classified into three groups depending on CT angiography criteria; these groups include:

Normal, stenotic lesions, total occlusion and non stenotic lesions. Stenotic lesions were further classified according to the percentage of stenosis to mild stenosis (1-29%), moderate stenosis (30-69%) and severe stenosis (70-99%).

رات
:om

CT angiography post processing techniques

CT angiography is noninvasive evaluation of carotid arterial disease. Maximum intensity projection (MIP) and shaded-surface display (SSD) mainly are used to create three-dimensional images of the vasculature **(Clude D. et al.,1999).**

The volume-rendering technique (VRT) has recently been used to display three-dimensional angiographic images when optimal display of the surface or internal detail was needed. The computer processing for VRT traditionally has been slower than for SSD and for maximum intensity projection display because the entire data set is incorporated into the final VRT image. Recent improvements in computer hardware and software have made VRT a more practical and rapid tool **(Xavier Leclerc et al., 1999).**

The combination of 3D CT angiograms and selected use of MPR images at the level of luminal narrowing appear to be an appealing approach that may also provide important information about plaque composition and remodeling and could easily be applied in clinical setting **(Roberto Corti.et al 2003).**

In our study (MIP), (SSD), (VRT), and (MPR) were obtained for each patient. The computer processing for VRT was slightly slower than for SSD and MIP displays, where MPR is the fastest processing technique.

رات
:om

Some authors consider that calcified plaque could be a limitation of CT angiography. This limitation can be avoided when multiplanar volume reconstruction is used, even when circumferential calcified plaques are present. An important advantage of MPR images is the ability to choose curvilinear reconstruction plans that skip vessel wall calcifications, rendering a precise definition of the lumen. Calcifications should not, therefore, be considered limitations of CT angiography **(Roberto Corti et al., 2003).**

Calcifications are the main limiting factor on MIP images owing to the inability to separate concentric calcifications from contrast material on these images. Volume rendering enabled accurate 3D evaluation of ICA stenosis despite the presence of dense calcifications **(Xavier Leclerc et al., 1999).**

In our study we have met seven carotids with calcified plaques and the stenosis was assessed by volume-rendering and MPR images with depiction of the residual lumen at the site of stenosis in these cases.

Helical CT has gained wide acceptance in the evaluation of a variety of traumatic and nontraumatic emergency conditions. High-quality diagnostic images are obtained in a short time; this is an essential factor to consider in critically ill patients. It also offers less discomfort for the patient and decreases costs. In the emergency setting, helical CT has gradually replaced traditional imaging techniques such as conventional angiography. (**Felipe Múnera et at., 2002)**

Transverse images are usually sufficient to make a proper diagnosis in most patients. Reformatted and three-dimensional images are complementary in complex cases. These images are also useful in planning the surgical procedure, since the surgeons usually preferred the reconstructions that more closely resembled the conventional angiograms. The postprocessing time was no more than 15 minutes. The capability to give information about potential associated lesions from such vital structures as the cervical spine and airway is an additional advantage that allows rapid triage of the patient. **(Pannone A. et al., 2000).**

Helical CT angiography is a nonoperator-dependent diagnostic study, and results can be easily reproducible in any trauma center by using established technical parameters. Helical CT angiography has also been used to plan large facial and neck reconstructions in trauma and oncology because it allows correct assessment of the vascular anatomy and the evaluation of blunt traumatic dissection **(Novelline RA et al., 1999).**

We evaluated helical CT angiography as an initial diagnostic test in patients who were hemodynamically stable and had penetrating trauma to the neck (**Felipe Munera et at., 2002).**

In our study we have met one patient with history of stab wound to the right side of the neck. CT angiography depicts an extravascular collection of contrast agent arising from the right common carotid artery, which represents a pseudoaneurysm with fistula to internal jugular vein. This findings show good correlation with color duplex sonographic findings

The percentage of stenosis.

The residual lumen at the lesion site is compared with the lumen at a reference site. The degree of occlusion is measured in terms of the diameter or area of stenosis **(Hideki Ota et al., 2005).**

Toshinori Hirai, has mentioned that, When the diameter of the lumen was measured at 3D CT angiography, we used the MPR images perpendicular to the longitudinal axis of the internal carotid artery at 3D CT angiography for the following reasons. First, the apparent diameter of the lumen may change with the angiographic display technique. Shaded-surface display can clearly depict 3D relationships by simulating light reflections. However, shaded- surface display images cannot display x-ray attenuation for values in structures within the threshold range. Although images with the maximum intensity

:om

projection and volume-rendering methods may be more accurate than those with shaded-surface display, the inherent accuracy of vascular depiction is strongly dependent on the parameters used to generate the angiogram-like images (eg, threshold value, window and level setting). Second, calcifications are the limiting factor on maximum intensity projection images owing to the inability to separate mural calcifications and intramural contrast material. To minimize this limitation, analysis in conjunction with transverse source images may be useful **(Toshinori Hirai et al., 2001)**.

Volume rendering enabled accurate 3D evaluation of ICA stenosis despite the presence of dense calcifications surrounding the residual arterial lumen. Calcifications are the main limiting factor on MIP image· The volume rending technique enabled the acquisition of angiogram-like images with 3D vascular interrelationships and a reliable estimation of the stenosis **(Claude D. et al., 1999).**

In our study we use advanced vessels analysis technique. (Software; GE Medical Systems). The most stenotic area and distal nonstenotic area were analyzed by acquiring multiplanar reconstruction (MPR) images at 3D CT angiography, depending on area diameter. The maximum stenosis was measured at each modality with North American Symptomatic Carotid Endarterectomy Trial criteria. And the results were

رات
:om

corresponding to the results of color coded duplex sonography. In addition, DSA which obtained for some cases shows a significant correlation with CTA results.

Length of stenosis

Also CTA can accurately shows the length of the stenotic segment even when it is sever as well as its sensitive in detecting ulceration **(Marks et al., 1993).**

In our study the length of stenosis is assessed by MPR as well as VRT, MIP and SSD and we have met three ulcerative plaques, and there was a significant correlation with color duplex sonography. Also DSA which obtained for some cases shows significant correlation with CTA.

Helical CT angiographic limitations include artifacts caused by metal, such as dental fillings or bullet fragments that may obscure arterial segments. In these cases, helical CT angiographic results should be reported as nondiagnostic, and these patients must undergo conventional angiography **(Dix JE et al., 1997).**

In our study we have met one patient with artificial metallic teeth, produced artifacts and obscured the upper cervical segment of internal carotid arteries.

رات
:om

Another limitation of helical CT angiography, as compared with conventional angiography, is the inability to perform therapeutic interventions with this method. However, helical CT angiography may be used to select patients as candidates for endovascular therapy such as embolization, prosthesis placement, or temporary vascular occlusion. CT angiography may be useful in identifying those who would benefit from surgical rather than endovascular treatment **(Dix JE et al., 1997).**

رات
:om

Summary and conclusion

The high incidence of catastrophic cerebrovascular disease all over the world and the wide spread prevalence of surgically accessible atherosclerotic lesion in the carotid vessels in such patients makes investigation and visualization of the carotid vessels especially the bifurcation of most importance.

This work aimed to evaluate the role of CT angiography in diagnosis of carotid artery disease. Normal carotid anatomy, pathology and basic physical principles and techniques of CTA were mentioned.

This study include 28patients (56 carotids) investigated with CTA. The examined carotid arteries were categorized into four groups depending on their CTA findings:

I- Normal carotid arteries
II- Stenotic carotid lesions.
III- Total occlusion group.
IV- Non-stenotic carotid lesions.

Stenotic carotid lesions were further categorized into three groups depending on the degree of stenosis:

I- Mild stenosis (1-29%)
II- Moderate stenosis (30-69%)

:om

III- Severe stenosis (70-99%)

We compare our results with color flow duplex sonography which obtained for all cases and digital subtraction angiography which obtained for some cases. From the results we can conclude that:

- CTA is a new developing technique that yields higher sensitivity, and non operator dependant than duplex sonography do. It less invasive and more economic than conventional angiography.

- The dominant limitation of CTA is attributed to the use of intravenous contrast that is contraindicated in sensitive and renal disease patients.

- CTA can be used in the diagnosis of carotid artery diseases including stenosis, occlusion, aneurysm and arteriovenous malformations. It can provide most of the information needed before carotid endarterectomy and thus alone or in conjunction with duplex sonography can reduce the need for preoperative carotid angiography.

رات
:om

References

- **Barnett HJ, Taylor DW, Eliasziw M. (1998):** " Benefit of carotid endarterectomy in patients with symptomatic moderate or severe stenosis: North American Symptomatic carotid Endarterectomy Trial Collaborators" N Engl J Med; 339:1415-1425.

- **Beck TJ**.**(1996)**: CT technology overview: state of the art and future directions. In: Gould RG, Boone JM, eds. Syllabus: a categorical course in physics-technology update and quality improvement of diagnostic x-ray imaging equipment. Oak Brook, Ill: Radiological Society of North America; 161-172.

- **Blum A, Walter F, Ludig T. (2000):"** Multi-detector CT: principle and new applications". J Radiol; 81 :1597-1614.

- **Boone JM. (1994)**: Computed tomography: technology update on multiple detector array scanners and PACS considerations. In: Andriole KP, eds. Practical digital imaging and PACS. AAPM Monograph 25. Madison, Wis: Medical physics Publishing; 37-63.

- **Bushberg JT, Siebert JA, Leidholdt EM, Boone JM.(1993)**:" The essential physics of medical imaging Baltimore", Md: Williams & Wilkins, 547-572

رات

:om

- **Brunnett CJ, Heuscher DJ, Mattson RA,and Vrettos CJ. (1994)**: CT design considerations and specifications. In: Gould RG, eds. Specification, acceptance testing and quality control of diagnostic x-ray imaging equipment. AAPM Monograph 20. New York, NY: American Institute of physics; 833-861.

- **Bruno Randoux, Béatrice Marro, Fabien Koskas,and Michel Duyme,(2001)"** Carotid artery Stenosis: Prospective Comparison of CT, Three-dimensional Gadolinium-enhanced MR, and Conventional Angiography." *Radiology*; 220:179-185.

- **Cortran R.B., Kumar V. and Collis T. (1999):** "pathological basis of desease " Saunder company, Piladelphia, Pennsylvania. Sixth edition: 498-507.

- **Cschieri A., Giles G.R. and Moossa A.R.(1995):** "Essential surgical practice". 889-904

- **Dix JE, Evans AJ, Kallmes DF, Sobel AH,and Phillips CD.(1997):"** Accuracy and precision of CT angiography in a model of carotid artery bifurcation stenosis". AJNR ; 18:409-415.

- **Elliot K.F. and Brooke R.J.(1998):** "Spiral CT principles and techniques and clinical application". Second Edition: 403-417

- **Felipe Múnera, Jorge A. Soto, Diana Palacio, Sol M. Velez, and Elcy Medina (2000): "**Diagnosis of Arterial Injuries Caused by Penetrating Trauma to the Neck:

رات
:om

Comparison of Helical CT angiography and Conventional angiography." Radiology;216:356-362.

- **Felipe Múnera, Jorge A. Soto, Juan E. Gutiérrez, and Giovanni García,(2002):** " Penetrating Neck Injuries: Helical CT Angiography for Initial Evaluation" *Radiology*;224:366-372

- **Fishman EK, Magid D. and Ney DR.(1991):"** Three-dimensional imaging". Radiology ; 181:321-337.

- **Fishman EK, and Kuszyk B.(2001):"**3D imaging: musculoskeletal applications". Crit Rev Diagn Imaging; 42:59-100.

- **Fox SH. (1995):** CT tube technology. In: Fowlkes JB, eds. Medical CT and ultrasound: current technology and applications. Madison, Wis: Advanced Medical Publishing; 349-377.

- **Haaga R.J., Chales F.L., Elias A.Z.and David S.S. (1994)**:'CT and MRI of the whole body". Third Edition: 519-523.

- **Hatsukami TS, Ferguson MS, and Beach KW. (1997):** "carotid plaque morphology and clinical events". Stroke; 28:95-100.

رات

:om

- **Heiken JP, Brink JA, Vannier MW (1997)."** spiral(helical) CT". Radiology; 109:56-91.

- **Hendee WR, Ritenour R. (1995)"** Medical imaging physics St Louis, Mo: Mosby, 1992. Hounsfield GN. Computerized transverse axial scanning (tomography)." Br J Radiol; 68:H166-H172.

- **Hideki Ota, MD, Kei Takase, MD, Hiroya Rikimaru, MD, Masahiro Tsuboi, MD, (2005)"** Quantitative Vascular Measurements in Arterial Occlusive Disease." Radiographics; 25:1141-1158.

- **Ho VB, Foo TK.(1998)**:" Optimization of gadolinium-enhanced magnetic resonance angiography using an automated bolus-detection algorithm". Invest Radiol; 33:515-523.

- **Hounsfield GN.(1995):"** Computerized transverse axial scanning (tomography). I. Description of system: 1973". Br J Radiol; 68:H166-H172.

- **Hu H, He HD, Foley WD,and Fox SH**. **(2000)**:"Four multidetector-row helical CT: image quality and volume coverage speed". Radiology; 215:55-62.

- **James O.D., Mcgree, Peter G. Isaacson and Nicholas A. Wright (1992):** " Oxford textbook of pathology" Volume 2a, Oxford university press, Oxford-New York-Tokyo;798-812.

- **Jerrold TB, Boone JM, and Edwin ML. (2002)**:"The essential physics of medical imaging: computed tomography".; 2nd edition. Philadelphia: Lippincot-Williams: pp 327-372.

- **Kalender WA. (1995):"** Thin-section three-dimensional spiral CT: is isotropic imaging." Radiology; 197:578-580.

- **Kathryn L. Mccance and Sue E. Huether (1994):** "The biologic basis for disease in children" Path physiology, second edition, Mosby : 100-10.

- **Kathryn L. Mccance and Sue E. Huether (1994):**"Spiral volumetric CT with single breath hold technique, Continuous transport and continuous scanner rotation" Radiology; 176:181-190.

- **Kuehne JP, Weaver FA, Papanicolau G, et al. (1996):** "Penetrating trauma of the internal carotid artery". Arch Surg 131:942-948.

- **Kumar V., Abul K. and Nelson F. (2005):** "Robbins and Cotran pathologic basis of disease".; Seventh edition :512-525.

- **Levy RA.(1995):"** Three-dimensional craniocervical helical CT: is isotropic imaging." Radiology; 197:645-648.

- **Lawler LP, Fishman EK. (2001):"** Multi–detector row CT of thoracic disease with emphasis on 3D volume rendering and CT angiography. RadioGraphics; 21:1257-1273.

- **Lewis MA. (2001):"** Multislice CT: opportunities and challenges". BJR; 74: 779-781.

- **Link J., Brossmann J., Penselin V., Gluere C.and heller M.(1997):**"common carotid artery bifurcation: preliminary results of CT angiography and color coded duplex sonography compared with digital subtraction angiography" AJR; 168:361-369.

- **Mahesh M. (2002):"** Search for isotropic resolution in CT from conventional through multiple-row detector". Radiographics 2002; 22: 949-962.

- **Mahesh M, Scatarige JC, Cooper J, and Fishman EK.(2001):"** Dose and pitch relationship for a particular multislice CT scanner". AJR Am J Roentgenol; 177:1273-1275.

رات
:om

- **Marek J., Mills I.L., Harvich L., Cui H. and Fujitani R.M(1996):** "Utility of routine carotid duplex in patients who have claudication" Journal of vascular surgery; 56:307-326..

- **Michael P.M., Sandy N., John E.J. and dieter R.E. (1993):** "Diagnosis of carotid artery disease: preliminary experience with maximum intense projection spiral CT angiography." AJR; 160:1267-1271.

- **Naylor AR, Rothwell PM, Bell PR. (2003):** "Overview of the principal results and secondary analyses from the European and North American randomised trials of endarterectomy for symptomatic carotid stenosis." Eur J Vasc Endovac Surg; 26:115-129.

- **North American symptomatic carotid endarterectomy trial collaborator (1991):**_"Beneficial effect of carotid endarterectomy in symptomatic patients with high grade carotid stenosis" N. Eng. J. Med.; 325:445-453.

- **Novelline RA, Rhea JT, Rao PM, and Stuk JL.(1999):"** Helical CT in emergency radiology". Radiology; 213:321-339.

- **Pannone A, Bertoletti** GB, **Nessi F, et al. (2000)**:" carotid artery dissection: correlation of different diagnosis techniques". Minerva Cardioangiol; 48:19-27.

- **Roberto Corti, Mario Alerci, and Rolf Wyttenbach. (2003):** "Usefulness of Multiplanar Reconstructions in

رات

:om

Evaluation of Carotid CT Angiography" *Radiology*; 226:290-292.

- **Rubin G.D., Michael D.D. and Charles P.S.(1995):** "Current status of three dimensional spiral CT scanning for imaging the vasculature ".Radiologoc clinics of North America; 33(1):51-58.

- **Rubin G.D., Shiau M.C., Leung A.N., et al. (2000):**"Aorta and iliac arteries: single versus multiple detector-row helical CT angiography" Radiology; 215:670-676.

- **Rydberg J, Kenneth A, Karen S, et al.(2000):"** Multisection CT scanning techque and clinical application". Radiographics; 20: 1787-1806.

- **Rydberg J, Liang Y, Teague SD. (2003):"** Fundamentals of multichannel CT. Radiol Clin N Am;41: 465-474.

- **Sameshia T., Futami S., Morita Y., Yokogami K., Miyahara S., Sameshima Y., Goya T. and Wakisaka S. (1999):**clinical usefulness of with three dimensional CT angiography for the evaluation of arteriosclerotic stenosis of the carotid artery: comparison with conventional angiography, MRA, and ultrasound sonography". Sug-Neural; 51(3): 3018-3089.

رات

:om

- **Scott W.W., Kenneth D.H., Thomas T.H., and Todd S.(1998):** "Measuring of carotid artery stenosis using CT angiography: the dilemma of artifactual lumen eccentricity". AJR; 170: 919-923.

- **Silverman PM, Kalender WA, Hazle JD. (2001):"** Common terminology for single and multislice helical CT". AJR; 176:1135-1136.

- **Taylor, D.C. and Strndress, D.E. (1987):"** Carotid artery duplex scanning".; J. Clinical ultrasound; 15:635-652.

- **Thomas G. Flohr, Stefan Schaller, Karl Stierstorfer, and Herbert Bruder (2005)**:" Multi–Detector Row CT Systems and Image-Reconstruction Techniques." Radiology; 235:756-773.

- **Thomas J., Guo Zhen Li., Wolfarm, and Kyung Mo Yeon(1995):"**Computed tomography future applications".; Springer velag Berlin Heidelberg:245-251.

- **Toshinori H., Yukunori K., Ken O., Yuka M. (2001):** "Maximum stenosis of extracranial internal carotid artery: effects of luminal morphology on stenosis measurement by using CT angiography and conventional DSA" Radiology; 221:802-809

رات

:om

- **Umberto D.G., Douglas C.A. and Matthew P.F. (1999):**"Robbin pathologic basis of disease".: Sixth edition: 498-507.

- **Walter J.B. and Talbot I.C. (1995) :** "Walter and Israel general pathology".; Seventh edition: 694-695.

- **Willian, Lawernce, Martin, Partica, Mary, Julian and Mark(1995):** "Anatomy of the carotid and vertebral ertery in Gray anatomy".;thirty eight edition: 15512-1526. Churchil Livingston, London.

- **Xavier Leclerc, Olivier Godefroy, Christian Lucas,and Jean-François(1999):** " Internal Carotid Arterial Stenosis: CT angiography with Volume Rendering" *Radiology*; 210:673-682.

رات

:om

ARABIC SUMMARY

رات

:om

الملخص العربى

إن انتشار الجلطات الدماغية على مستوى العالم مع التوسع فى امكانية العلاج الجراحى جعل فحص الشريان السباتى ذا أهمية قصوى.

استهدف هذا العمل دراسة دور ألأشعة المقطعية الحلزونية فى تشخيص امراض الشريان السباتى. وتضمن هذا البحث وصف تشريحى للشريان السباتى وشرح ألأشعة المقطعية الحلزونية وطريقة فحص الشريان السباتى.

ولقد اجريت هذه الدراسة على 28 حالة،17 من الذكور و11 من الاناث، وتم تقسيمهم تبعا لنتائج الفحص الىأربعة مجموعات.

- I- مجموعة ليست بها اصابة
- II- مجموعة بها اصابة تمثل ضيق بالشريان السباتى
- III- مجموعة تعانى من انسداد كامل للشريان السباتى.
- IV- مجموعة بها اصابات اخرى ليست بضيق .

وتم تقسيم المجموعة الثانية الى ثلاث مجموعات .

- I- مجموعة بها ضيق قليل الشدة (1-29%).
- II- مجموعة بها ضيق متوسط الشدة (30-69%).
- III- مجموعة بها ضيق اكثر شدة (70-99%)

وقد تم مقارنة النتائج بنتائج الفحص بطريقة موجات دوبلر فوق الصوتية التى تم عملها لجميع الحالات وبنتائج فحص الأوعية الدموية بالصبغة التى تم عملها لبعض الحالات.

رات
.com

وقد استنتج من هذا البحث ان الفحص عن طريق ألأشعة المقطعية طريقة جديده تمتاز بانها اكثر دقة ولا تعتمد على من يقوم بها مثل الموجات الصوتية كما انها اقل تكلفة وخطورة من فحص الأوعية الدموية بالصبغة ولكن يعيب استخدامها عدم ملاءمتها لمرضى فرط الحساسية ومرضى الكلى.

نلخص من هذا أنة بامكانية ألأشعة المقطعية تشخيص أمراض الشريان السباتى مثل الضيق والانسداد والتمدد الدموى وغيرها وانة يمكن استخدامها بمفردها أو بمساعدة الموجات الصوتية كبديل لفحص الأوعية الدموية بالصبغة قبل اجراء عمليات الشريان السباتى.

رات
:om

دور الأشعة المقطعية الحلزونية فى تصوير و تشخيص أمراض الشريان السباتى (خارج الجمجمة)

رسالة مقدمة من
الطبيب / محمود ابراهيم الشامى
بكالوريوس الطب والجراحة- كلية الطب-جامعة الأزهر
توطئة للحصول على درجة الماجستير فى الأشعة التشخصية

تحت اشراف

الأستاذ الدكتور/ مصطفى فاضل سنبل
أستاذ الأشعة التشخيصية
كلية الطب
جامعة الأزهر

الأستاذ الدكتور/عمرو محمود زايد
أستاذ الأشعة التشخصية
كلية الطب
جامعة الأزهر

الأستاذ الدكتور/هانى حافظ شريف
أستاذ الأشعة التشخصية المساعد
كلية الطب
جامعة الأزهر

كلية الطب
جامعة الأزهر
٢٠٠٥

رات
.com